**Department of Precision and Microsystems Engineering**

# Influence of Automated Fiber Placement in Fused Deposition Modelling with reinforced thermoplastic materials

Christian Mora Benítez

Report no : 2022.005
Coach : Dr. Can Ayas
Professor : Dr. Can Ayas
Specialisation : MSD
Type of report : Master thesis
Date : 31-01-2022

Delft University of Technology

**Master of Science**

in Mechanical Engineering

# Influence of Automated Fiber Placement in Fused Deposition Modelling with reinforced thermoplastic materials


*Author:*
Christian Mora Benítez (Student No. 4725573 )

*Supervisors:*
Dr. Can Ayas (TU Delft)
Joep Grapperhaus (10-XL)

*Thesis committee:*
Dr. Can Ayas (TU Delft)
Prof.dr. Fred van Keulen (TU Delft)
Dr. Angelo Accardo (TU Delft)


January 31, 2022


# ABSTRACT

Fused deposition modeling (FDM) is one of the fastest-growing additive manufacturing processes in recent years. Nevertheless, the mechanical properties cannot be matched to those of traditional manufacturing methods such as injection molding.The research presented in this report aims to demonstrate the limitations of fusion deposition models and proposes automated fiber placement (AFP) as a way to mitigate them by improving transversal tensile strength and elastic modulus.

The background and main characteristics of the stated processes, as well as the state of the art, are discussed in this paper. It is explained how both methods were integrated for a production line built specifically for the execution of this research. The key parameters are listed, along with their impact on the end part.

Mechanical parameters such as tape-to-print bonding strength, tape-to-tape bonding strength, molding unidirectional fabric tensile strength, and 3D printed part tensile strength were all compared in the experiments. The major challenges to be addressed are surface roughness, print-to-tape contact area, and heat transfer when taping, according to the results. Yet, there is still a large potential for these methods to achieve better performance.

# Contents

# 1 Historical Context

Additive manufacturing (AM), is a term used for those manufacturing methods in which, unlike traditional methods that are based on removing material to give the shape, the material is added in different ways, sometimes it is also referred to as 3D printing and is considered by many as the third industrial revolution[45].

This type of innovative manufacturing was born in the late 1980s with the founding of two main companies, 3D Systems and Stratasys in the United States of America. The first, 3D systems, was born with the creation of the stereolithography method which is not within the scope of this project but it is worth understanding its fundamentals. Stereolithography (SLA) is a process that allows the formation of complex pieces that, through localized photopolymerization process and with the help of UV radiation solidifies liquid monomers, oligomers, and photoinitiators layer by layer to give the final shape. With this first manufacturing method, the era of Additive manufacturing began.[25]

Later, in 1988 Stratasys was born, founded by Scott Crump and his wife, who initially sought to create a figure using a glue gun and a mixture of different plastics and wax. Once this experiment was successfully carried out, he decided to take it to a more industrialized process thus creating the first 3D printer with a patented process that he called Fused Deposition Modeling. [38, 47]

This method became popular during the 1990s especially for those fans of Do-it-Yourself (DIY). Since it was a process that allowed them to create parts at a very low initial investment cost of machinery and raw material. During this same decade and the following, new additive manufacturing methods became popular and were standardized by ASTM as can be seen in the following image:

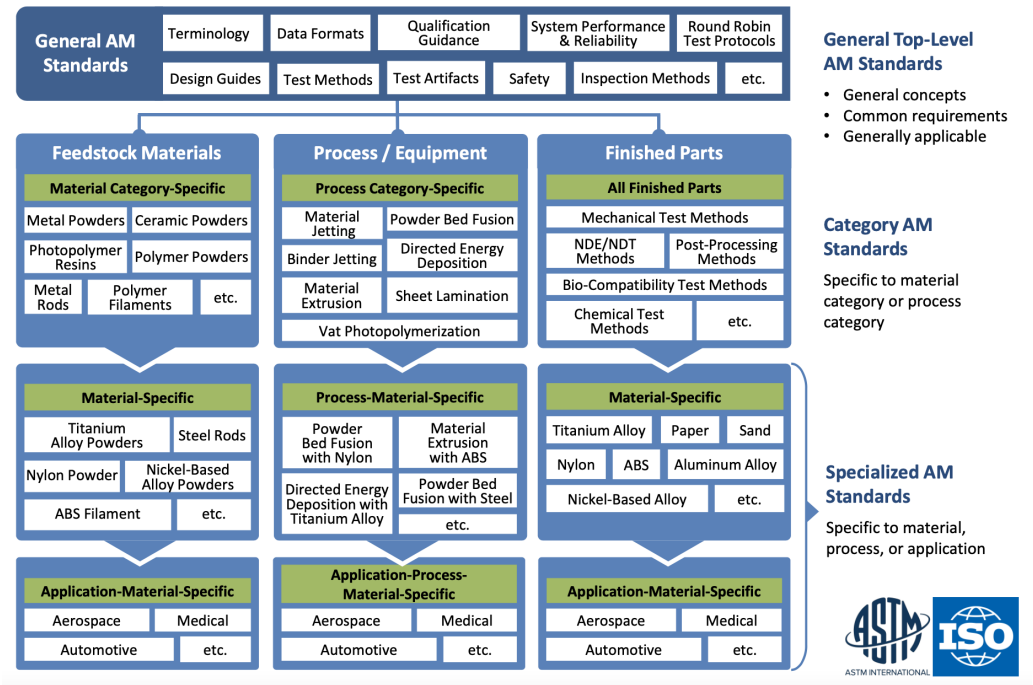


Figure 1: ASTM Standards Structure for additive manufacturing processes[5]

In summary, Additive Manufacturing processes fabricate parts by creating successive 2D layers

to form a 3D object [22]and is divided into seven main methods: Material Jetting, Binder Jetting, Material Extrusion, Vat Photopolymerization, Powder Bed Fusion, Directed Energy Deposition, and Sheet lamination. The materials used in these methods include polymers, metals, ceramics, and composites. [45]

The only one that is within the scope of this research and will be mentioned in the following chapters is Material Extrusion since this is where FDM and automated fiber placement fall. Due to weight constraints and material costs, high-performance thermoplastic materials and applications are not the research's goal.

Aerospace applications that require a mold to perform Automated Fiber Placement (AFP) that later is removed when the procedure is completed are excluded. These should also not necessitate any modifications beyond the conventional FDM and AFP processes.[45]

# 2 State of the Art

## 2.1 FDM

Fused deposition modeling (FDM) is one of the manufacturing processes with the greatest growth in recent years, it has been adopted and evolved more than any other Additive Manufacturing process. It has gained popularity due to its low cost, flexibility, ability to create complex and lightweight geometries. It consists mainly of a heated nozzle whereby a filament, commonly a thermoplastic material, is heated until it becomes semi-molten and then is extruded and deposited layer-by-layer on the working bed, and the set of these 2D layers will give the final shape of the 3D geometry. [22, 45]

There are many benefits of AM that companies have seen, a greater efficiency in design and production times as well as a reduction in costs in their supply chain. This is due to the flexibility of being able to create designs more quickly between each iteration and with complex geometries that other traditional methods do not allow. One of the greatest successes of FDM and the AM processes has been the possibility of quickly and effectively prototyping, customizing and testing before being able to make a large outlay of money in the creation of the tooling for its production.[7, 17, 18]

FDM is a Crump proprietary term also known as Fused Filament Fabrication (FFF). The main characteristics and attributes of the process will be covered in greater depth during the next sections.

## 2.2 Types of 3D Printers

This technology also became popular thanks to the small size of printers and their ability to generate prints in a matter of minutes in homes and small businesses. The first printers were used to create prototypes for applications within the home and small workshops or offices.

For industrial applications, larger printers have been developed that, depending on the industry, it has become common to use metallic, plastic, and ceramic materials. Depending on the sector, the size, material, and shape of the printers vary radically. In the aerospace industry, metal FDM has been a significant factor for weight reduction and geometry optimization, in a commercial metal 3D printer is shown.

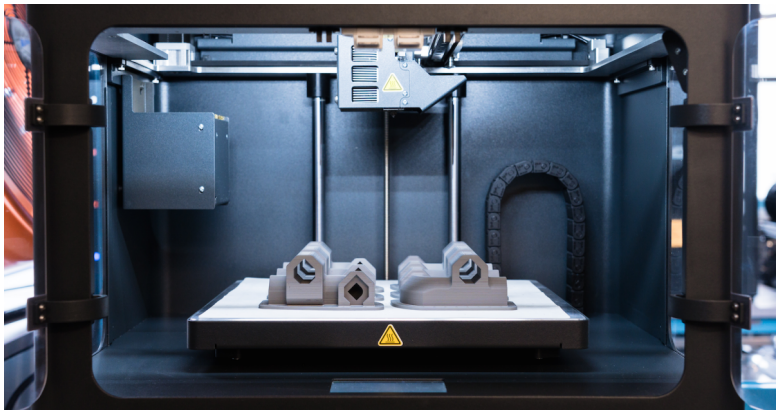

Figure 2: Markforged metal 3D printer [31]

The printers can be divided into 4 groups according to their shape and the coordinate system employed for position and movement, these are Cartesian, Delta, Polar, and SCARA.[1, 4, 41]:

### 2.2.1 Cartesian

Even though the name of this group refers to the coordinate system it uses, it differs from the other groups given the form of a gantry-like structure. It consists of 3 degrees of freedom or x, y, and z-axis where one axis remains constant during the printing of each layer, z, while the movement occurs in the other two and at the end of the layer the z-axis advances to the height of the next layer. This type of printer is the most commonly used in small size commercial 3D printers given its ease and low cost. However, it is also often used for large prints and the main advantage is to be more accurate, consistent, and better quality prints due to the rigidity of the structure allowing a smoother and more precise movement.

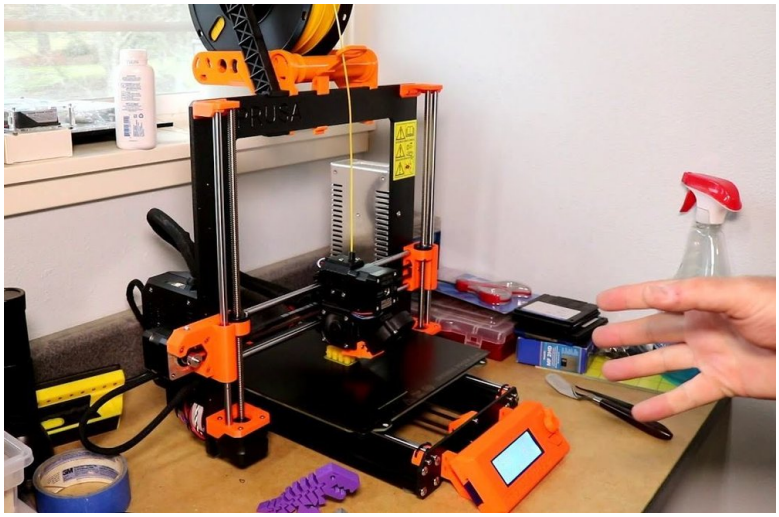

Figure 3: Cartesian printer [1]

### 2.2.2 Delta

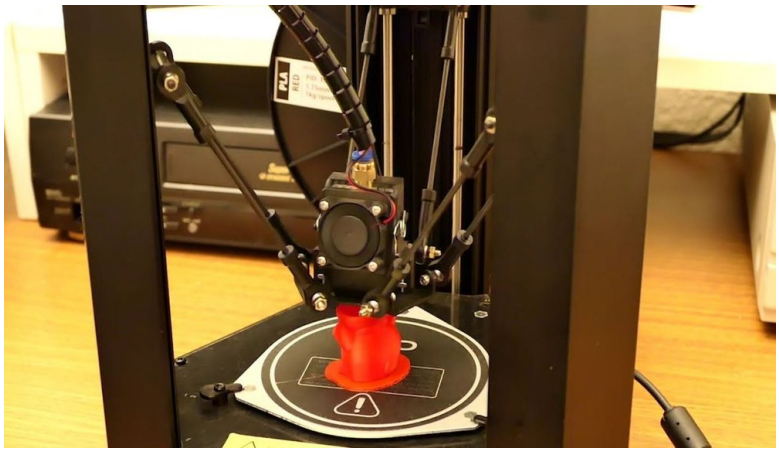

Figure 4: Delta printer [1]

Like the previous group, it has 3 degrees of freedom but the difference radicate in the nozzle movement. The nozzle is supported by three arms in rails, being able to move at the same time providing the nozzle greater flexibility while the working bed remains fixed, its main advantage is the speed that can be reached due to a lighter nozzle system compared to a cartesian printer. A comparison between these two can be seen in Fig. 5.

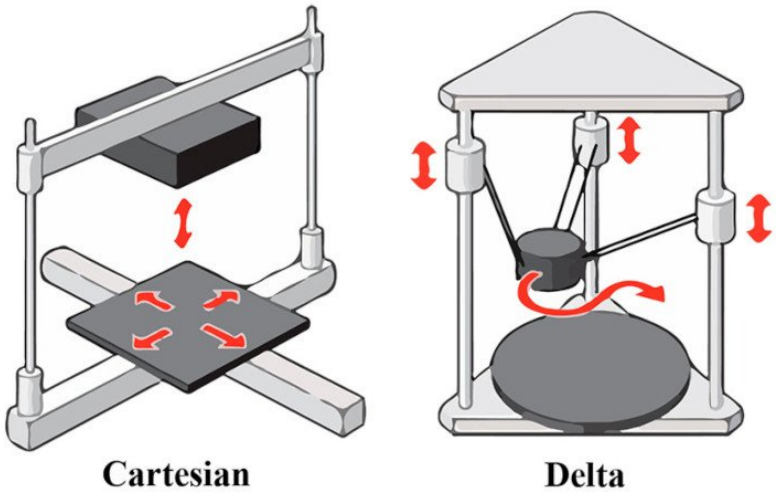


Figure 5: Cartesian vs Delta printer [41]

### 2.2.3 SCARA

Selective Compliance Assembly Robot Arm (SCARA)[1] has great flexibility given the common usage of industrial robots nowadays. Any robot of any size can be adapted for use as a 3D printer. The main difference with other cartesian FDM printers is that the motion system involves the usage of multiple arms that enable the printer to rotate around the X and Y axis, in addition to the linear movements of traditional printers allowing it to follow more complex paths. As will be mentioned in the next stage of the project, this configuration will be used to obtain the study samples and results.

Figure 6: SCARA printer [41]

### 2.2.4 Polar

It is the only group that does not use the Cartesian coordinate system, on the contrary, as its name indicates, it uses the polar system. Each point is specified by its distance and angle with respect to the center of the working bed while the nozzle is supported by a sigle arm.

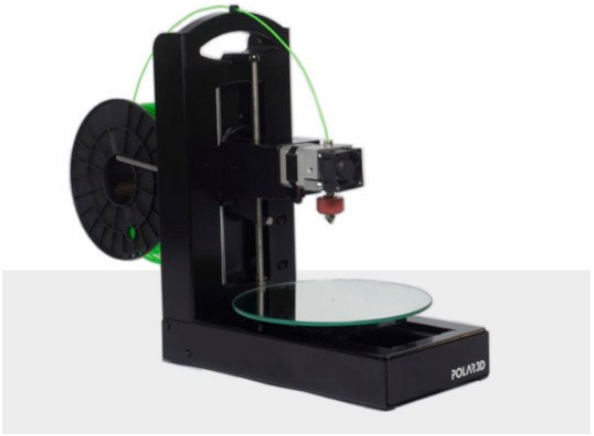


Figure 7: Polar printer [41]

## 2.3 Thermoplastics and Fiber-Reinforced composites

The most commonly used materials in FDM are ABS (Acrylonitrile Butadiene Styrene), PLA (Polylactic Acid), PA (Polyamide), and Nylon because of their low melting temperature.[22, 45] The extrusion's average temperature range for these materials goes from 180 to 260º.

These same materials are employed as a matrix in fiber-reinforced composites and reinforced with continuous or short carbon, glass, or Kevlar fibers, which have excellent inherent mechanical qualities. These composite materials have also been made with nanoparticles, a combination of polymers, and chemical procedures, resulting in improved mechanical, electrical, thermal, optical, and other properties.

Recently, the development of new composites and biocompatible materials has made it possible to expand their use to medical applications, automotive, aerospace, wind energy, food, and high-

performance demanding industries. Within this, composite materials with wood, graphene, and stem cells stand out. [28, 45]

## 2.4 Main Characteristics

When talking about 3D printing or FDM, it is necessary to mention the main attributes that characterize it. Among them are:

**Dimensional Accuracy.** Simply explained, it's the difference in size between the designed and real printed parts. Several factors influence: printing orientation, cooling gradient, layer height, geometry complexity, and infill, among others. One of the main problems for Dimensional Accuracy is warpage, which occurs when one layer is deposited and then cools until the following layer is formed and re-heats the preceding one. Internal stresses emerge from the temperature difference between the layers, causing warpage or delamination and causing deviations to the designed part.

**Surface roughness.** the surface quality of the print is determined by the height of each layer commonly called *Stair case effect* [38], it is one of the inherent characteristics of additive manufacturing processes that create the layer-by-layer shape and one of the main challenges to overcome, different approaches to tackle this problem will be mentioned in Section 3.1.2.

**Mechanical strength characteristics.** It is related to inter-layer bonding and the infill percentage. More information on mechanical properties in Section 3.

**Build time.** the manufacturing time for an individual part according to the printer speed, part size, layer height, support requirements and build orientation.

## 2.5 FDM process flow

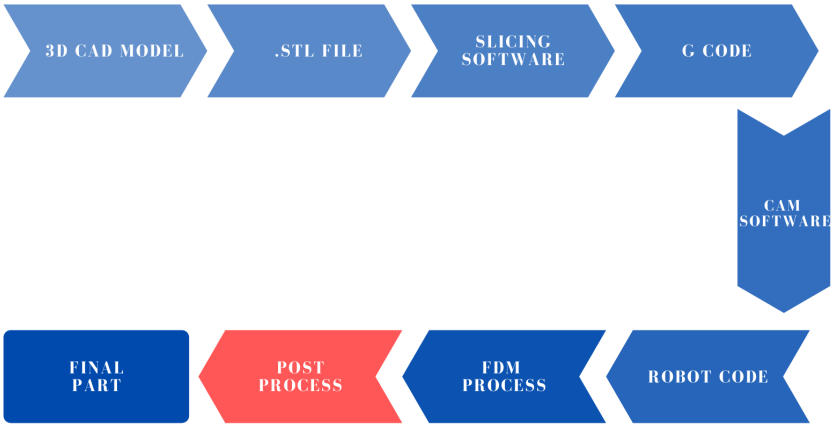


Figure 8: FDM process flowchart adapted from [7, 14, 17, 18, 45]

In Fig. 8 it is possible to see the general process for FDM from the design of the 3D model to obtaining a physical part. Throughout this section, the different stages of the process and the expected outputs will be explained.

### 2.5.1 3D Design CAD


Figure 9: CAD [7, 14]

The first step of the FDM process is the creation of a 3D model through the use of computer-aided design (CAD) software. [17] Currently there are various software that allow us to create and export these models. The most used are Solidworks, Rhinoceros 3D, Fusion 360º although there are many more.

**Output:** STL File

### 2.5.2 .STL File


Figure 10: STL File [7, 14]

The CAD-based 3D model is typically saved as a standard tessellation language (.STL) file, a mesh representation of the model divided by triangles. Although there are also other more recent formats such as .AMF (Additive Manufacturing File) that seeks to attack the limitations of .STL files, in Section 3.1.4 a deeper description about these limitations is done. [17, 45]

### 2.5.3 Slicing Software


Figure 11: Most used slicing software [23]

At this step, the .stl file is divided into layers to obtain a G-code and according to Ultimaker, one of the world's leading printer manufacturers, *G-code is a language that humans use to tell a machine how to do something, this type of code gives the machine the commands where and how to move* [42]. This series of commands results in the toolpath to follow to achieve the final geometry by the printer.

For home use commercial printers, the manufacturer provides the software that directly slices the part and transforms it into a code capable of being understood, and CAM (Computer-Aided-Manufacturing) Software is not required.

**Output:** Gcode including toolpath

### 2.5.4 CAM Software

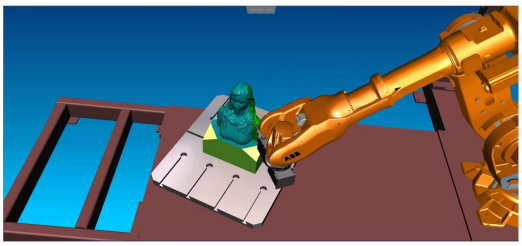

Figure 12: CAM Software Eureka [19]

In industrial applications, Computer-Aided Manufacturing software is necessary. As mentioned in Section 2.2.3, this type of software is focused on SCARA style printers. To control a robotic arm, each manufacturer has its series of commands, so it is important to note that the language varies between each of them.

This type of software allows us to transform the G-Code into a robot code, which can be translated by the robot controller and also takes into account the limitations of the work area, such as obstacles, degrees of freedom, and working area.

**Output:** Robot Code

### 2.5.5 AM Process

Figure 13: FDM process

Here the actual AM process takes place, the printer by depositing material, according to the toolpath created previously, creates 2D layers on top of the previous one, the set of these 2D layers gives the final shape to the 3D part. [17].

**Output:** 3D physical object

### 2.5.6 Post-Processing

Figure 14: CNC Milling post-process [34]

There are different types of post-processing, commonly used are CNC Milling, Drilling, Gluing, Painting. These Post-processes aim to compensate for the defects inherent to the FDM process as introduced in Section 3.4.

**Output:** Enhanced 3D physical object

# 3 FDM Challenges and Gap of Knowledge

One of the main challenges of FDM, like all additive manufacturing processes, is to at least match the properties of traditional processes such as injection moulding. [18]However, in recent years, there has been a push to not just equal but to outperform them, which, when combined with the fundamental benefits of these methods, could accelerate their adoption for large-scale commercial applications.

In order to overcome the challenges, it must be understood that the mechanical properties of the final part can be affected by the properties of the materials as well as the manufacturing method used. That said, in this section, an overview of the challenges and drawbacks will be provided.

## 3.1 Challenges

### 3.1.1 Mass manufacturing

There are three main obstacles for FDM to be considered a process for mass manufacturing. The first is the limitation in the materials that are commercially available now. This range is limited by the capabilities of existing printers both by the reachable temperature as well as the final parts' dimensions. An example of this problem is the compatibility of materials between different brands that due to the filament materials or the fiber reinforcement materials that are used can block the nozzles if the parameters are not adjusted correctly. [28]

On the other hand, the building time of this type of process is significantly longer than that of traditional manufacturing processes, which generally increases the costs associated with production. The third one is the print quality and structural reliability that are explained in-depth in Section 3.1.2 and Section 3.1.3, respectively.

### 3.1.2 Surface quality and Dimensional Accuracy

Two qualities are searched in an FDM process in terms of geometry and finishing. Surface quality is related to layer height and is a trade-off with printing time. To have high resolution it is necessary to make the layer height as small as possible but this has a direct impact on the building time, the shorter the height, the more layers will be needed to reach the same final height and therefore, it will take a longer time to be printed. Section 3.4 mentions novel methods to combat these imperfections.

The second is Dimensional Accuracy, also known as print tolerance. In a few words, it is the difference when comparing the original model versus the printed one. There are tolerances defined according to the industry for which the model is directed, in the high-performance industries that tolerance is very small and something that FDM still struggles with. In the early days of this type of technology, it was not so important to be so precise, unfortunately, if the objective is to create parts for end-use, it is necessary to be able to achieve high resolution. [22]

### 3.1.3 Material heterogeneity and structural reliability.

*3d-printed parts are weaker under tension than in compression*[18], Design for Additive manufacturing is changing the way of traditional design, the main goal is to achieve better quality with minimal anisotropy and lower mechanical asymmetry. Parts created with FDM systems

suffer from anisotropic mechanical properties due mainly to a higher modulus and strength in the direction of the deposition lines. Likewise, The bonding of bordering lines in the horizontal plane will vary particularly with the local process conditions, material properties, and stress concentrations related to non-uniformities of the deposited fiber caused by the temperature gradient.

The ratio of tensile strength to compressive strength, also known as tension/compression asymmetry, could be up to 50%, i.e. compressive strength could be up to 50% higher than the tensile strength, making FDM the AM process with the largest ratio. [18, 22, 29]

Short fibers or continuous fibers are added to the matrix to improve the mechanical properties but the lack of control over the orientation of fibers supplied to the matrix material is one example of how a part's heterogeneity is impacted.

According to Dizon et al., there is still not enough literature regarding the behavior of additively manufactured parts, more research must be done to be embraced by the industry. Furthermore, for this technology to be adopted at a commercial and industrial level, it is necessary to create standards that regulate and test structural and mechanical acceptability, spotting here the anisotropic properties inherent to these processes. These standards will establish the foundations and guidelines to make the processes more reliable, safer, and repeatable. [18]

### 3.1.4 Software

3D Design software plays an important role in the process, currently using a file extension that was created for stereolithography has many areas to improve. Usually, this type of file represents the design in polygonal meshes or tessellations, the most common is unstructured triangular, however, this carries resolution problems, self-intersection, gaps, and cracks that make the algorithms of the slicing software unstable and can even cause the total failure in manufacturing. [13]

G-code generating software, also known as slicing software, has many limitations and is continually being improved to make it more robust and memory efficient.

## 3.2 Industry

Not all are negative points, it has seen a positive impact by AM in small companies, entrepreneurs, and clients since the design, prototyping, and manufacturing process is simplified and cheaper, which leads to faster innovation. Worth noting that this is due to the low investment costs for this type of technology and the variety of materials available is increasing every day.

It has also managed to catch the attention of larger companies as an opportunity for cost reduction within their supply chain, including warehousing and delivery, acknowledging AM's flexibility to produce on-site and on-demand [22] and the waste generated, which at the same time reduces cost on materials.

Even when it is possible to see several advantages of these manufacturing processes, advantage must continue to be studied and developed to replace traditional processes. Calignano et al. allude to the fact that the development of this technology is negatively affected given the limited collaboration among industry and academia, a greater interaction through the two is necessary to close the gap between needs and solutions.

## 3.3 Summary of drawbacks

FDM creates 3D printing parts with a layered microstructure that can be seen as a transversely isotropic material, i.e. the properties depend upon direction. There is a difference in properties in the inter-layer, exterior, and in-between material, creating different defects. In between layers, inter-layer material, it is more common to find voids that lead to porosity. In addition, Software approximation errors and the staircase effect due to layer-by-layer deposition are the biggest challenges for FDM.

All these features help to comprehend the anisotropic properties, a tension/compression asymmetry regardless of the material or specific AM process, and these drawbacks reduce the mechanical performance and require more research to overcome to finally be widely adopted by industries. In this regard, the increased funding, research, development worldwide, and market pressure would result in a fast transition from traditional methods. [33, 40, 46]

## 3.4 FDM defects and mitigations

Methods to compensate for drawbacks are mainly focused on improving the bond between the matrix and the reinforced fiber. Improving the chemical bond among the fiber and matrix leads to improved inter-laminar shear strength by the elimination of voids and is commonly done, as mentioned by Sai and Yeole, by post-processing the printed part to increase the adhesion between neighboring fibers via thermally driven diffusion.[18, 38, 40, 43, 45]

Here are some novel methods proposed by Wickramasinghe et al. to compensate for these defects in Additive Manufacturing processes that are not exclusive to FDM:

**1) chemical treatment process** As an additional process, acetone is often used to dissolve the outer surface of the part to eliminate voids and gaps created by the staircase effect. This method dissolves the matrix, filling the spaces through the layers, improving the surface roughness by up to 97%, although it negatively affects the mechanical properties. This process can be done during or after printing. During printing, it is carried out in a controlled atmosphere with nitrogen gas and significant improvements of up to 30% have been seen in tensile strength. [18, 45]

**2) Laser treatment process** Uses the same principle mentioned above of filling the pores on the surface by melting the matrix with the help of a laser. Unlike a chemical process with a solvent, with optimal conditions, it is possible to improve the surface quality and tensile properties at the same time. [45]

**3) Heat process treatment** Thermal annealing increases the interlayer adhesion of polymers, improving tensile strength and outperforming injection moulding. [45]

**4) Ultrasound treatment process** This process is mainly used during the printing process to reduce the staircase effect increasing the layer adhesion, therefore, the tensile strength but it can be also applied before, where the polymer matrix and the fiber are joined resulting in a better coating of the fibers.

As can be seen, the pursuit to reduce defects is mainly focused on improving the surface roughness and eliminating voids by filling them with the polymer matrix. Consequently, even when there is an improvement in some properties, the tensile strength is still not comparable to

traditional methods; most of these post-processes must be discarded due to their nature, cost, and complexity for large parts.

## 3.5 Gap of knowledge

*'Printed parts have a long and notorious history of being significantly weaker than their production counterparts.' Brown [12]*

Even though commercial printers can create thermoplastic parts with a higher strength-to-weight ratio than traditional methods and metal parts, tensile strength remains weaker along the printing direction, z-axis, and this is accentuated with greater height. That is why processes such as those mentioned in Section 3.4 are applied to improve the mechanical strength of the parts. [12, 18, 43]

To date, research has been focused on improving printing through the development of new materials or composites with the addition of fiber reinforcement. Initially with short fiber and more recently with continuous fiber reinforcement, which, although it has been seen a significant improvement, does not fully tackle the lack of stiffness in the printing direction, hence anisotropy remains.

The second line of research has been pre-processing, among which stand out pre-heating with laser or infrared light. The principle is to preheat the extruded layer (existing layer) closer to the glass transition temperature before the next layer is deposited, improving interlayer bonding strength. This can be ensured by different kinds of light sources such as laser or infrared light. [43]

According to research done by Syrlybayev et al., it has been possible to see an improvement but without conclusive results, that is, depending on each particular case, the material used, and specific setup, it is necessary to find the appropriate values to see a significant improvement and it is not possible to establish a clear ratio of how significantly the mechanical properties of the print could improve.

In conclusion, an additional process must be added to tackle the shortcomings of FDM. In the next section, a process will be proposed as a solution to the aforementioned defects, to prove that FDM with some enhancements can have similar or even better mechanical characteristics than traditional processes such as injection moulding.

# 4 Closing the gap

This project proposal aims at filling the gap between prototyping and manufactured end products. Therefore, it will try to answer the research questions:

RQ1 *Is it possible to overcome the drawbacks of Fused Deposition Modeling (FDM) adding Automated Fiber Placement (AFP) process?*

RQ2 *How do AFP process affect the final part?*

This paper seeks to fill the space between the design and modeling of prototypes and the manufacture of finished and usable products. Today various lines of research seek to improve the mechanical properties of parts created with FDM. An example is the multi-material 3D printers, which allow, in addition to introducing short or continuous fibers to the polymer

matrix, to control the types of materials used and therefore their composition and properties. This mix of materials allows to create objects with a gradient of functionalities and properties by combining materials with contrasting properties. [28]

The development of new composite materials has given the possibility of reaching new sectors in which these additional manufacturing processes can be adopted. As Kalsoom et al. *"In the area of composite design and production, 3D printing represents a technology with immense potential, providing low cost, simple and rapid prototyping advantages over traditional methods for fabrication of composite materials and objects "*. However, the goal of this project is not to improve the materials or find a mixture of them to find the required properties, but to combine two manufacturing processes that until today have not been used in this way.

In sum, this project aims to propose a novel combined process of FDM and AFP where the combination of both improves the mechanical characteristics of the printed parts and give the process window for the main parameters involved.

# 5 Automatic Fiber Placement

## 5.1 Historical background

Automated tape placement is a promising composite forming technique that involves the fusion bonding of a prepreg tape to a substrate. A laminate part can be obtained, avoiding an extra process of autoclave, within a single process by heating the interface between the incoming tape and the substrate and exerting pressure, making the technique appealing to industry. The material must go through multiple subprocesses to achieve in-situ consolidation: heating, consolidation, and cooling. [30]

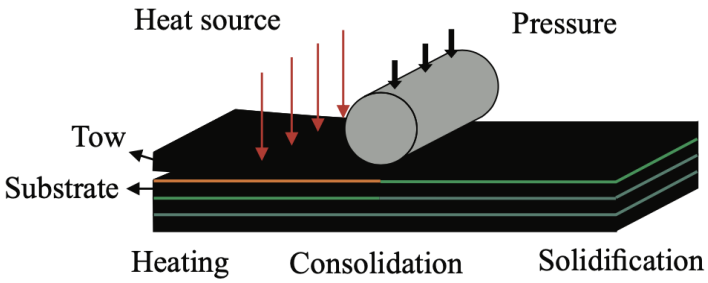


Figure 15: AFP general process schematic [30]

These are generally semi-automated or fully automated procedures for producing composites or preforms with continuous fiber reinforcement on curved or flat surfaces.This method was developed in the 1960s to create complicated, lightweight, and corrosion-resistant airplane fuselage structures. The processing of thermoset prepregs was initially the focus, but it was later expanded to include thermoplastic semi-finished products and bonded materials. In the 1970's decade, Ingersoll Milling Machine Company supplied the first commercially functional line. Fiber placement has been used in several industries since the early 1990s, and countless components have already been fabricated utilizing this technology.

When compared to thermoset fiber-plastic composites, the following broad benefits are apparent: unlimited shelf life, processability in non-conditioned environments, autoclave-free pro-

cessing via inline consolidation, excellent impact properties, exceptional chemical resistance for semi-crystalline thermoplastics, fusible, formable, weldable, short processing cycles and solvent-free processing are all possible.

The polymer chains can diffuse through the boundary zone if the contact surfaces are merged. Autoadhesion is a polymer physics phenomenon in which the mechanical twisting/bonding of freely moving molecule chains generates a mechanically strong link.[6]

In the production of thermoplastic composite parts, it is extremely critical to achieve good quality using only the fiber placement procedure and avoid the need for an extra process, autoclave, to reduce production-related costs. However, due to the numerous elements and parameters involved in the AFP process, reaching the desired quality of the AFP-produced part is difficult. In previous research done by Shadmehri et al., it was found that manufacturing parameters such as temperature, compaction force, also known as consolidation pressure, and layup speed have a significant impact on the quality of fiber-reinforced thermoplastic composites.

These three parameters can be considered as the main or most critical but some others will be mentioned later. The goal of this paper is to understand the effects of each parameter on the final mechanical properties and if it is possible to determine which one influences at a higher degree. To have a better understanding, different tests are proposed, the setup and results will be discussed in Section 7.

AFP technology is mainly intended for high-performance industries such as aerospace, where it is required to lighten the weight of the parts as much as possible. However, this type of process is usually very expensive due to the type of machinery and materials used, mainly carbon fiber. Therefore, this project does not target those industries that require a lower weight regardless of cost, but those that seek complex geometries with the benefits of FDM but that manage to reduce the cost and improve their properties, making this process viable for commercialization to a medium volume and pass the prototype stage to be both technically and financially viable.


Figure 16: AFP Cell, working bed adapted with vacuum system for flat taping

AFP has been widely studied as a stand-alone process, consisting of the application of layers of prepreg tapes of carbon or glass fibers pre-impregnated with thermoplastic or thermoset resin matrix materials.

The process consists of a tape placement head that heats the prepreg tape, regularly using a hot gas torch, infrared, or laser as a heat source, and with a compaction-roller press it against the surface or mold to give the final shape, also known as in-situ consolidation. [35]

Recently Bahar and Sinapius and Raspall et al. have investigated the use of AFP with 3D printing, the objective is to help the AFP process reduce defects when positioning the layers and cover the gaps that can be created by the machine errors, in other words, using FDM as a secondary or supporting process. It has not been possible to identify in literature an investigation where fiber placement is used as a complementary process to FDM.

## 5.2 State of the Art

### 5.2.1 Laser

Currently, many of the companies that are involved in the construction of parts for the aeronautical industry use a laser as a heat source. The main advantage of this system is the ease of controlling the power of the diode, and the heat distribution is quite good. However, this type of source cannot be used for materials such as glass fiber due to its refraction index hence, it is

mainly used for carbon fiber tapes. Another of the drawbacks of this process is the need for a dedicated installation to carry out this process safely since a closed-cell that blocks the laser is required, and the system operators must stay away from the line when it operates. This makes the initial cost higher on top of the already high price of the laser.

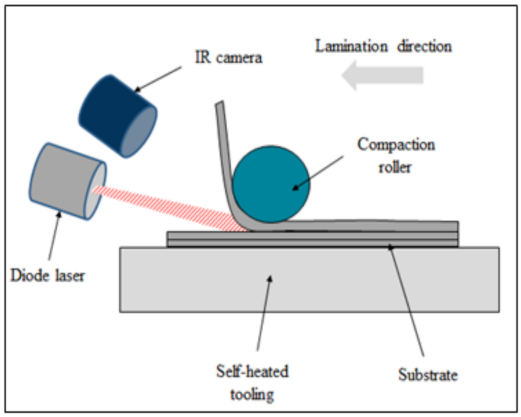


Figure 17: AFP Laser - Heat source [32]

### 5.2.2 Hot gas torch

This system is characterized by using gases at high temperatures to transmit heat to the tape. The disadvantage of this system is the low efficiency to transmit in a homogeneous, constant, and fast way, which prevents it from being used at high speeds. Among its main benefits are the low initial investment required and the ease of operation.

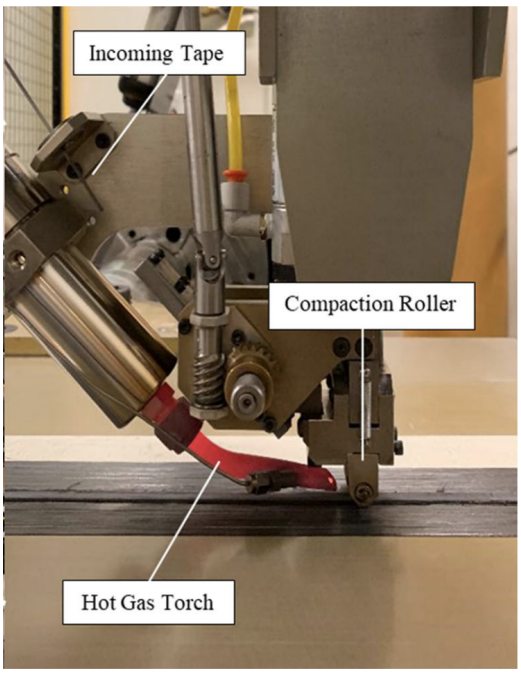


Figure 18: AFP Hot gas torch - Heat source [3]

### 5.2.3 Flame Torch

Unlike Hot gas torch, which uses hot air, with a Flame torch there is direct contact between the tape and the flame created from the gas mixture. The most common gases used for these

systems are hydrogen, nitrogen, and oxygen. The temperatures with which they operate vary between 900°C and 2800°C. [6].

This type of system is between the two mentioned above in terms of cost, but above them in terms of the speed that has been achieved. Although the installation and operation of this tool have high safety requirements, it is still below those necessary for lasers, which makes it an attractive option for the industry.

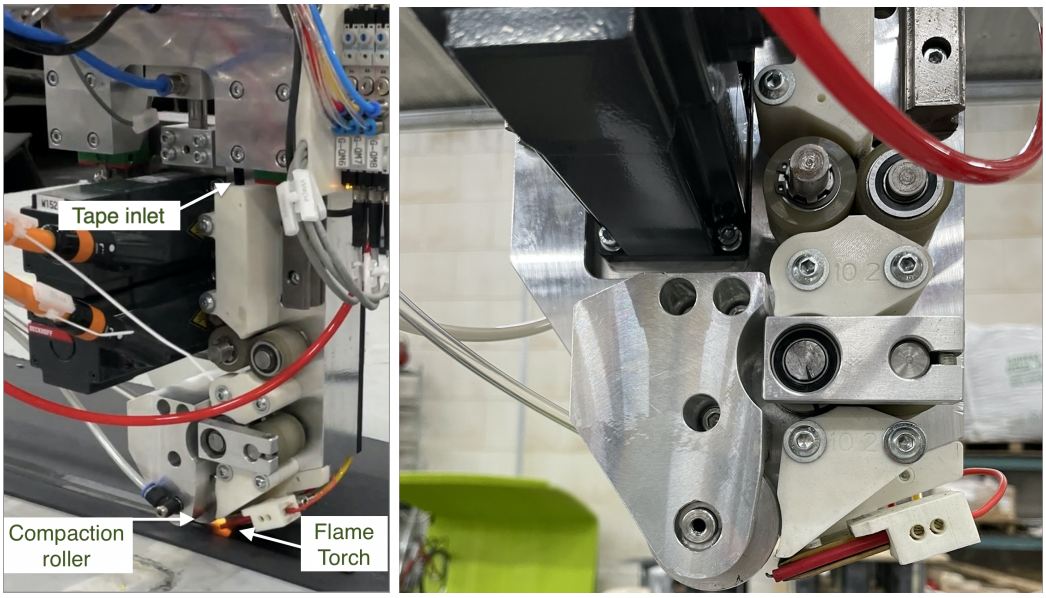


Figure 19: AFP Flame torch - Heat source

## 5.3 Process Parameters

As Baz Radwan remarked, *'Understanding those variables and their interactions in relation to each other as well as how their variances affect the quality of the product, will allow for a better control of the process.'*

The three primary parameters that influence the process are mentioned in Section 5.1, and each of them will be discussed more below:

- Placement speed (v) The layup speed, also known as feed rate, determines how quickly the tows are deposited onto the tool surface or substrate. As a result, it is the most important indication of the process' productivity. Maintaining a fast layup speed while preserving part quality and consistency during automated layup is challenging.

  There is a trade-off between these parameters, i.e., there is a strong link between them. For example, the layup speed will dictate how long the tows are exposed to the heat source. In case a higher speed is demanded, a higher heat level must be ensured to guarantee that the matrix melts and bonds to the surface or previous tape.

  It was mentioned by Baz Radwan that a 50% reduction in layup speed resulted in a 50% reduction in the number of gaps at a placement speed of 127 mm/sec. Lower rates may result in higher layup quality, but can also result in over-compaction or heat damage. Setting a target speed that corresponds directly to the desired production rate and finding

the process window for the other parameters in respect to this speed is the strategy followed for the tests done during this research.

- Processing Temperature (ºC)

  Processing temperature is specific to each process and material, in the Fig. 20 it is possible to see the general temperature window for thermoplastic tapes. Finding the optimal temperature for the tape used and the number of layers is key to ensuring the quality of the final part, with increased speed, thermal degradation reduces, in the opposite, too-high speed leads to ineffective bonding.

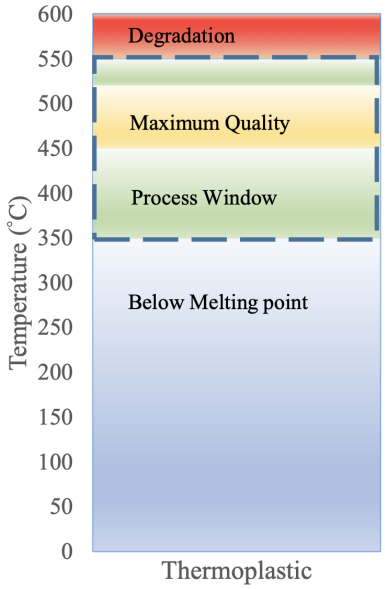


Figure 20: Effects of temperature on Thermoplastic tapes [11]

- Consolidation pressure ($\rho$)

  Insufficient pressure causes adhesion loss, increased void content, and wrinkling in the case of steering. Over-compaction might result in liquid components from the tape leaking onto the surrounding surface. It is also noticeable a relationship between layup speed and compaction pressure, with lower rates requiring less compaction force. If processing is to be done at a high layup speed, a safe method would be to utilize a high value of compaction. An alternative solution was proposed, using a soft rubber roller boosted the pressure uniformity by 50% and reduced void content by 92%.[11]

- Secondary Parameters: There are many more factors that influence the AFP process, recent studies have found that the impact is not as great as the ones stated above. Nevertheless, there is a link with the primary parameters, that can cause flaws and anomalies.[6]

  - Fiber volume content (Fvol%)
  - Tape thickness (d)
  - Tape width (b)
  - Melting viscosity of the matrix material (Tl)

– Steering radius (r) or path curvature

## 5.4 Process anomalies and limitations

Previously, the main and secondary parameters were discussed and given their correlation, these can directly influence the following limitations and can occur due to the effect of one or a combination of them.

During this section, limitations and defects that can occur during the process as well as their main characteristics will be mentioned. More detailed information can be found in [24, 35]:

- Overlap: An overlap is when the two adjacent tows are overlapping onto each other. [24]
- Gaps: A gap is when two adjacent tows are not perfectly laid up next to each other and there is a gap between the two.

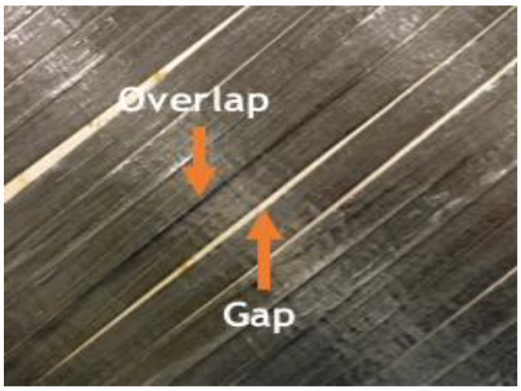


Figure 21: Gap and Overlap representation [24]

Research was conducted to investigate the effects of these gaps on performance and the results show that gaps lower strength while overlaps boost local strength. [35]

- Wrinkles are generated by tows being placed at a small steering radius, resulting in an extreme difference in length between the two edges of the tow's bow on the component surface. After compaction and curing, these types of flaws appear on the inner radius and remain out-of-plane.

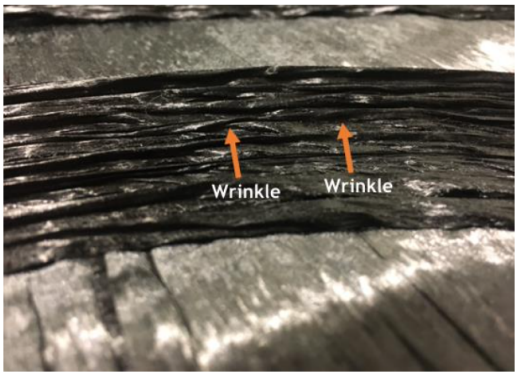


Figure 22: Wrinkle representation [24]

- Bridging - Occurs when a bridging tow does not entirely adhere to the concave surface over which the tows are laid up, a gap between the radius of the concave tool surface and the tow appears, a physical representation can be seen in Fig. 23. The most common reasons for a bridged tow are excessive towing tension, which causes the tow to lift up, and insufficient tack adhesion to the surface being built upon due to the roller not making complete contact with the substrate material.

Figure 23: Bridging representation [24]

- Steering: Can cause the above-mentioned anomalies, when utilizing AFP, there is limited debate on the effect of process parameters on steering. When producing steered courses, process parameters like temperature and feed rate can have a significant impact on the presence and distribution of irregularities.

  To avoid these drawbacks, it is necessary to test the turning radius for the tapes to be used. Depending on the width of the tape, the turning radius may be larger or smaller and, coupled with the process temperature and placement speed, have a significant impact on the presence and distribution of irregularities.

- Thickness vs plies: When designing the part to be produced, a FEM analysis is usually performed to determine if the stability of the structure and stress distribution and plan a taping strategy. This taping strategy will determine the time of the process, generally, tapes ranging from 0.1-0.25 mm are used but the thickness depends on the application and line setup.

  When defining the taping strategy it is necessary to understand the trade-off between the number of plies and the thickness of the tape. When using a thinner tape, the number of plies will be larger to obtain a similar result. Likewise, by requiring a greater number of plies, the total taping time will increase considerably, the same occurs when selecting the width of the tape.

- Divergent geometries: The geometry influences the taping strategy. When aiming to make an AFP process to a divergent section, inherently, if the objective is that the entire surface is covered, overlaps will be generated. Simplifying the geometry, if possible, will prevent the formation of defects.

- Surface Roughness: surface roughness is important for bond strength development at the interface since resin must flow through dry fiber bundles to create effective intimate contact, more dry fibers on the tape's surface would prevent the creation of effective intimate contact while decompacted fibers increase the surface roughness. [15, 30, 32]

Results reported by Çelik[15] show that reducing the heated length of the tape or increasing the placement speed, while keeping the nip point temperature constant, are two heating tactics that result in fewer dry fibers at the surface.

- Thermal degradation Thermal degradation of a polymer is a process in which an irreversible loss of physical, mechanical, or electrical properties happens as a result of the impact of heat or high temperature. At extremely high temperatures, the polymer undergoes deterioration, resulting in cavities at the surface that cannot be compensated for in subsequent passes, lowering the strength values.[32]
- Speed and TCP constant Gantry systems and articulated robots are commonly used, which must accurately accelerate and break a load ranging from 750 kg to 25 t along the travel path, in combination with the application unit. The physical approach $force = mass * acceleration$ can be used to calculate the required drive power. During the accelerating and braking stages, the application speed is not constant, therefore, a runaway distance and overtravel are required. The ratio of driving power to move mass must be adjusted and carefully regulated.[6]
- Residual stresses: The release of residual stresses in the thermoplastic tape is linked to two types of deconsolidation: increased surface roughness from fiber decompaction and the creation of waviness. These stresses are introduced to the thermoplastic tape during the manufacturing process when individual fibers or fiber bundles are stretched, squeezed, or bent, and then held once the resin solidifies.[15]

## 5.5 AFP Process flow

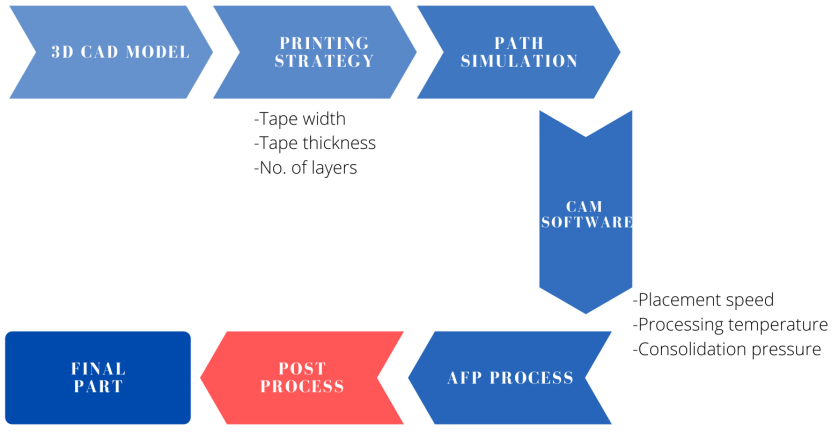


Figure 24: AFP process Flowchart with main parameters

The general process of automated fiber placement is illustrated in the image Fig. 24. First, it is necessary to have the 3D model of the geometry to be processed to insert it into CAD Software that can be standalone or a plug-in for the most used software such as Catia or Rhinoceros 3D. In this step, the taping strategy will be created where the characteristics of the tape and the number of plies used are necessary. In general, this type of software has a simulator where it is possible to preview the path that the tool head will follow.

With the help of a post-processor or CAM software, the design will be translated into a code capable of being read by the robot and the tool head controllers.

There are proposals for post-processes to improve the quality of the final part, nowadays reheating with an air gun is used that specifically seeks to reduce the surface roughness and improve the bonding layer to layer, but processes after tape placement are not part of the scope of this project.

The path followed by the taping tool head shown in Fig. 25 consists of three sections: approach, taping segment, and departure. In Section 6.3 it is explained in more depth how the integration between the FDM and AFP processes was carried out for this project.

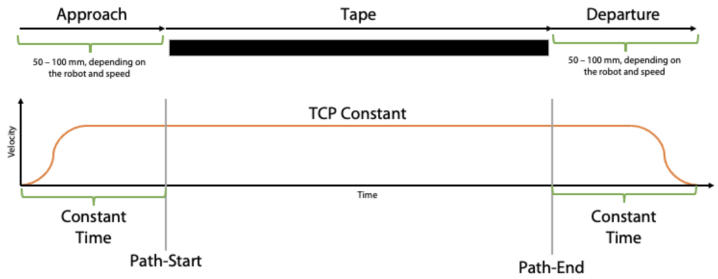


Figure 25: Taping path depiction

## 5.6 Usages

Recognized companies such as Coriolis Composites, which have been involved with Automated Fiber placement for some time, have supplied production lines for the manufacture of renowned aircraft such as Bombardier C Series, Airbus A350, Airbus A320NEO, Russian MS21, ships, and auto parts. There are also companies in the automotive and aeronautical industries that have adopted this technology, among them we can find Airbus, Ariane Group, Bombardier, Dassault Aviation, PSA, Safran, Stelia Aerospace, TAI, or Turkish Aerospace.[16] In Fig. 26 we can see one of the lines created by Coriolis for the manufacture of fuselages.

A combination with FDM would allow the adoption of this technology for the manufacture of boats, bridges, and wind turbines, as well as the use of multi-materials, Thermoplastics-Metals, and the broad applications that it could lead.

Figure 26: Coriolis AFP system for aircrafts demonstration [16]

## 5.7 AFP + FDM Main advantages

The main commercial advantages that the combination of these two manufacturing processes has concerning moulding are listed below:

- Flexibility:
  - Allows design improvements without having to make a new mold.
  - Decentralization of production and on-site production capacity.
- Cost:
  - Less waste of raw material generated, therefore lower cost.
  - It is not necessary to manufacture different molds if there are diverse parts to be manufactured
  - Less space required
- Time: Companies are still doing moulding by hand, which takes more time added to the time for curing the material for the thermoset.
- Space efficient:
  - Raw material storage
  - Less productive area required
  - No storage area for molds needed

## 5.8 Software & Simulation

For this project, it was decided to use the ADDPATH plug-in for Rhino, since it complies with the minimum requirements specified by the taping tool head's manufacturer: Tool center point constant speed and analog input/output for triggers. The first is essential to achieve optimal

heat distribution, while the second, as will be explained later, allows the connection between the robot and tool controllers.

There were other determining factors for the choice of this software, among which the easy collaboration of the company stands out since the CEO has graduated from TU Delft, created the company recently and this allowed the integration process to be smooth. Likewise, the cost of the software is significantly lower than that developed by companies with a longer time on the market.

Among the main characteristics of the plug-in, it is worth mentioning the automatic and manual path generator, simulation, and post-processor that allow the CAD software Rhino to simulate the work cell to avoid collisions, simulation f the process to have the first preview, detect possible errors and correct them prior to the actual process and finally, extract a code already supported by the ABB Robot that was used.

In Fig. 27 an image of the plug-in where the cell designed specifically for the line installed in the 10-XL facilities as well as the different adjustable parameters of the process is shown. More information can be found directly on the developer page ADDCOMPOSITES. [2]

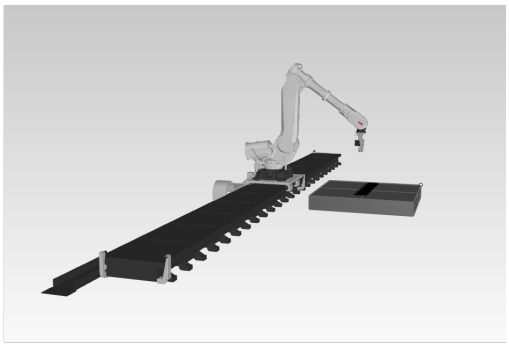

Figure 27: 3D model of 10-XL production cell

## 5.9 AFP Conclusions

In this section, the main parameters, secondary parameters, limitations, challenges, and anomalies of the AFP process have been reviewed. In conclusion, this in-situ consolidation method for thermoplastic composites manufacture is a difficult balance between the high temperatures required for local melting and healing of the substrate and incoming tape surfaces while avoiding material thermal degradation and optimizing for processing time.[11, 32]

The three main parameters: placement speed, processing temperature, and consolidation force must be adjusted individually for each type of material and taping strategy to find the process window and set the foundation for industrial production. Even though some of the benefits and the great potential that it has have been demonstrated in some research, it is necessary to understand more deeply and accurately the characteristics and adjustable settings to be able to bring this process to large-scale production.

# 6 Problem statement

The objective of this project is to allow the creation of new products for the startup 10-XL from the Fused Deposition Modeling process. To achieve this objective, it was necessary to think about how to improve the mechanical properties in such a way that one can go from a prototype to a final product, thus solving the problems inherent in this additive manufacturing process.

To achieve this expansion into new industries, a new independent taping line was visualized at the company's facilities. Currently, there is an FDM production line to print parts up to 12 meters, Fig. 28. To be able to use both processes at the same time it was decided that the line would be installed separately with the option of being able to add other additional processes to the taping line later on.

## 6.1 FDM production line

This production line has been in operation for approximately 5 years and has printed boats, bicycle stations, outdoor furniture, statues, among many other things. As mentioned, this line has a movable platform that allows creating prints up to 12 meters long and the flexibility to use various materials.

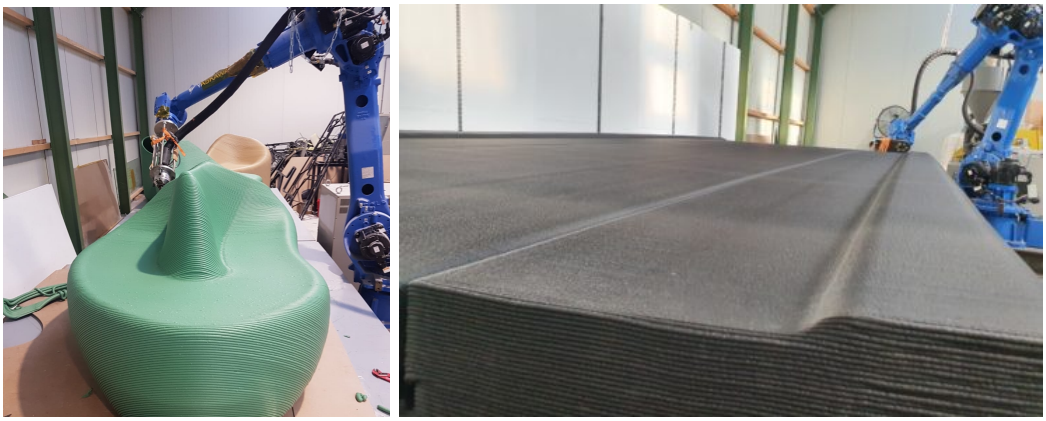

Figure 28: FDM production line at 10-XL

## 6.2 AFP production line

The production line for Automated Fiber placement was installed for the development of this research and its intention is to be one of the largest AFP production lines in Europe. With a vision to make the process for large-scale products, an ABB robot with a reach of 3.20 m was installed on an ABB track that allows the robot to slide up to 12 meters(Fig. 29).

Figure 29: ABB Robot and 12-meter long track installed at 10-XL

Once the robot and track were installed and integrated, the taping tool head was incorporated. Unlike some that exist in the market, the company opted for a German supplier that manufactures a tool of reduced size and with great versatility.

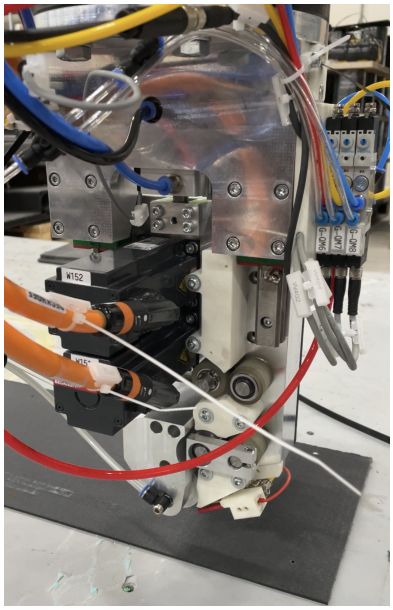


Figure 30: Taping Tool head

This device combines oxygen and hydrogen as fuel to create a flame that melts the polypropylene in the tape and achieves proper adhesion. Specifically, this form of heat source was chosen because the tape and printing substance did not allow the usage of lasers due to its refractive index, rendering this type of technology unsuitable.

It has been feasible to exceed the speed of other laser-based tools in tests conducted by the

manufacturer with a setup different from that described in this work, reaching speeds of up to 4 m/s.

## 6.3 Automated Fiber placement line Integration

The tool's creation and integration with the robot were done in collaboration with ADDCOMPOSITES, the developer of the Rhino plug-in, and the manufacturer of the tool head. We can observe the flow of the process in the Fig. 31, where there are two branches to manage the process. On the one hand, this is where the FDM process is combined with the geometry of the printed part using ADDPATH, the software used to generate the taping strategy Section 5.8

The code is obtained owing to the post-processor activated in ADDPATH particularly for the ABB IBR6640 Robot, which provides analog and digital signals to define its location: Approach, Path, or Departure as shown in Fig. 25, and is controlled by the position of the TCP. This integration is critical for the controllers to work together correctly and for the tape path to be followed precisely.

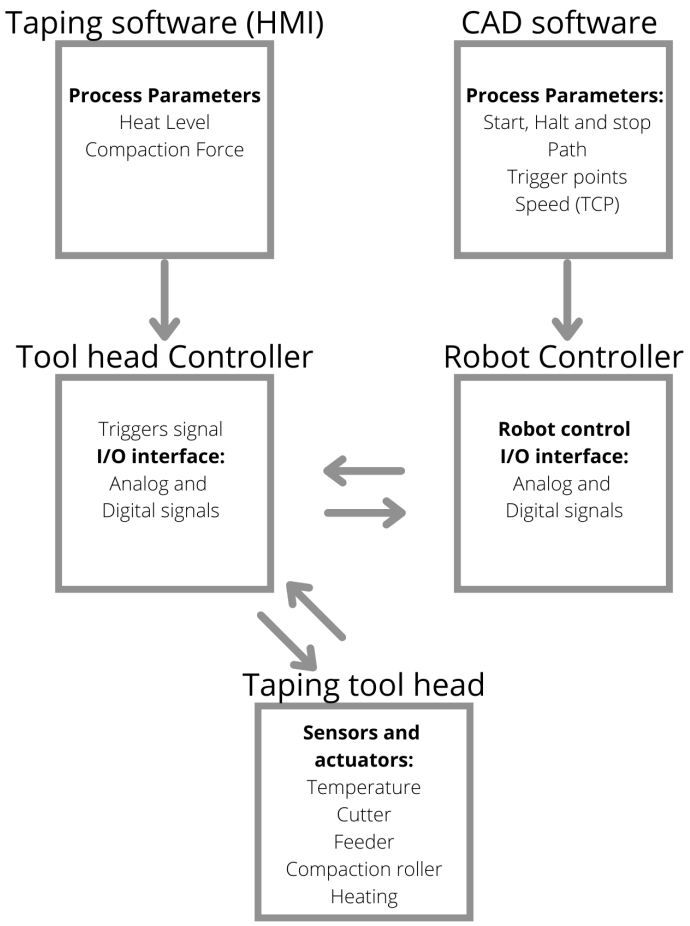


Figure 31: Automated Fiber Placement and Robot Integration flowchart

## 6.4 Mechanical properties expectations

It is intended that the mechanical properties, as mentioned previously, are at least equal to the moulding process with which the functional parts are currently manufactured. The main ones to compare in this research are Elastic modulus and $\sigma_{\max}$.

The current values of the parts created with moulding are:

- $\sigma_{\max}$: 700 [MPa]
- Elastic modulus: 30 [GPa]

While combining these two processes, however, there are some crucial aspects to consider when setting the process parameters: The properties of print to tape bonding strength and tape to tape bonding strength will be discussed further in the next section and in Table 1. It's worth noting that these factors have no counterpart in the moulding process, thus there's no direct comparison.

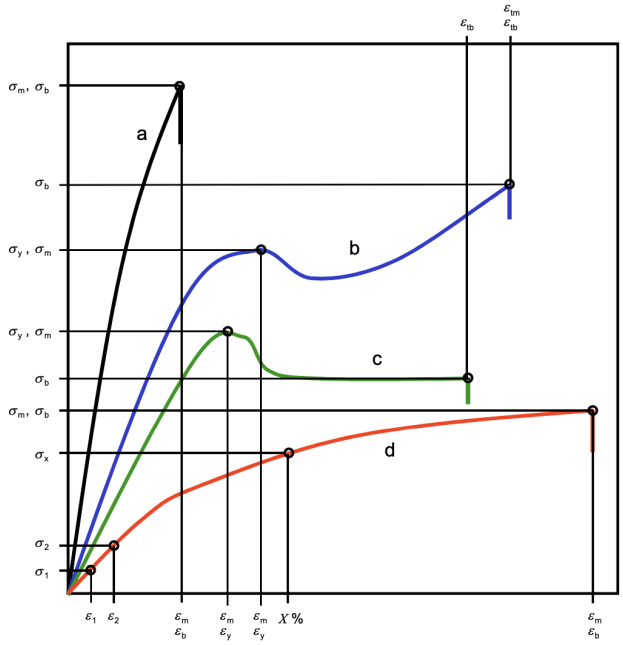


Figure 32: Typical Strain-Stress curves - Curve (a) represents a brittle material, Curve (d) represents a soft rubber like material breaking at larger strains. [27]

Due to the brittleness of the Polypropylene matrix of the specimens, a Strain-Stress curve similar to a) from Fig. 32 is anticipated. In other words, the elastic component dominates the tensile test graphs, while the plastic component is minor or non-existent before the rupture.

# 7 Test setup

## 7.1 Test Plan

The tests performed, as well as the standards that each of them was based on, will be discussed in this section. The goal is to establish a point of comparison between the current moulding process and the novel FDM proposal combined with AFP, as well as to determine how the key

AFP parameters affect the final features. Although, some tests do not have an analog for the traditional approach, but are critical for taping, were carried out to understand the influence of the parameters.

The specimens manufactured for the following experiments were created at 10-xl facilities where the inherence of the different associated parameters has been investigated over 5 years. For these tests, it is aimed that in the printing the defects that were mentioned in Section 3 do not appear or in the least amount possible, specifically, it seeks to reduce the surface roughness and keep a layer height as small as possible to increase the contact surface. The parameters used are the following:

The Experiments were carried out at Howden's facilities in the Netherlands, while the AFP process was carried out in-house. The tests performed including the strength to be tested, are listed in the table below.

| | **Characteristic to test** | **Sample configuration** | **Quantity** | **Sample Extraction** |
|---|---|---|---|---|
| **Test A** | Print-tape bonding | Single lap shear | 15 | Sawing |
| **Test B** | Tape-tape bonding | Peeling | 15 | Shorten with scissors or knives |
| **Test C** | Taping angle | Single lap shear | 9 | Sawing |
| **Test D** | Tape as received | Tensile test | 6 | Shorten with scissors or knives |
| **Test E** | Print interlayer bonding | Single lap shear | 3 | Sawing |
| **Test F** | Moulding process | Tensile test | 3 | Sawing |
| **Test G** | Printing angle | Tensile test | 8 | Waterjet |

Table 1: Summary of tests performed

## 7.2 Materials

Thermoplastic composites are becoming more popular as construction materials; the possibility of a phase transition in a viscous, near-liquid matrix state in the case of a high-temperature effect is a unique feature of such materials. [20]

The testing panels were printed with Transmare 3D printing compound Polypropylene, 50 percent glass fiber for this project. The density and Melt flow index are 1330 kg/m$^3$ and 8 g/10min, respectively. FRT tapes Unidirectional glass-reinforced and polypropylene-based with 0.25 mm thickness, density is 1670 kg/m$^3$ and 45 percent fiber volume percentage were also utilized. [21, 44]

During the research performed by Rijsdijk et al., results suggest a relation between longitudinal and transverse properties of continuous-glass-fiber reinforced polypropylene composites as 5-8% for the tensile modulus and tensile strength. This approximation is used to get $E_{22}$ for Tape and Moulding fabric while for the printed part is obtained experimentally.[37] Accordingly, the properties are shown in the next table:

| Modulus | 3D printed PP GF30 | Prepreg tape | Moulding fabric |
|---|---|---|---|
| $E_{11}$ **[GPa]** | 1.54 ($0^{o}$) | 37 ($0^{o}$) | 30 ($0^{o}$) |
| $E_{22}$ **[GPa]** | 0.59 ($90^{o}$) | 5%*$E_{11}$ = 1.85 [37] | 5%*$E_{11}$ = 1.5 [37] |
| **v** | 0.3 | 0.3 | 0.3 |
| $\rho$[kg/m$^3$] | 1330 | 1670 | 1650 |
| **thickness [mm]** | 4 | 0.25 | 1.5 |

Table 2: Print compound, tape and Moulding UD fabric mechanical properties, where: $E_{11}$=longitudinal tensile modulus, $E_{22}$=transverse tensile modulus, v=Poisson ratio.

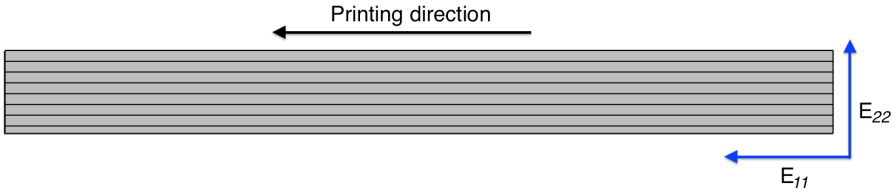


Figure 33: $E_{11}$ and $E_{22}$ tensile modulus orientations according to the printing direction

The values shown in Table 2 come from the Data sheet for more information can be obtained from Appendices A.1 and A.2. [21, 44]

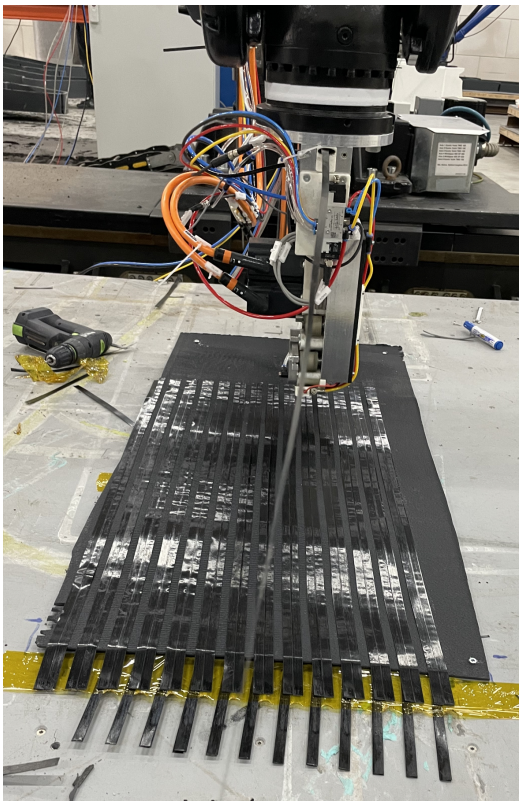

Figure 34: FDM printed panel for testing samples extraction

## 7.3 Parameters evaluation

Different experiments were carried out to identify the optimal parameters, in which the variable to be evaluated was increased while the others remained constant. First, it was determined what the robot and track's speed constraints were, and then a comparison was made between different degrees of compaction force and heat source.

- Compaction force: Tool head software's range from 0-300 N
- Heat level: Gas flow through the torch measured in nanoliters per minute in the range 0-5 nL/min.
- Taping speed: set inside ADDPATH plug-in, within the range 0-1000 mm/sec.
- Overtravel: After laying the tape, the tool goes a certain distance to ensure that the total distance is compacted.
- Runaway distance: To keep the TCP speed constant, the tool must approach and attain the final TCP speed before beginning the taping path.
- Approach speed: Usually lower than the placement speed to avoid damages if a collision occurs.
- Minimum taping length: due to the distance between the tape feeder and the cutter, there is a minimum amount of tape to be placed.

### 7.3.1 Taping speed selection

To find the optimum parameters, a test was first performed to determine the maximum speed that the robot and tool head could achieve. The first test was performed at a speed of 250 mm per second, and the results were satisfactory. Later, the speed was increased to 500 mm/s, and it was easy to add 16 plies of 0.25 mm thickness without difficulty, allowing the speed to be increased even further.

The optimal speed was determined based on a visual inspection of the surface finish; while a significant difference between one speed and another was not observed in the surface finishing and tape to tape bonding, speed was increased. It's worth mentioning that with a gantry configuration, the tool head we're working with can reach a maximum speed of 4,000 mm/s (4 m/s), meaning that the inertia of the robot and track is the most significant constraint.

According to the results obtained during the tests at various speeds, the existing setup produces satisfactory results at 250 mm/sec and 500 mm/sec, yet the bonding between the tape to print part and the tape to tape was not suitable at 750 mm/sec since it detached during handling. Thus, for the tensile tests, the optimal speed is fixed at 500 m/s.

### 7.3.2 Compaction force and Heat level

In total 15 samples were made with the characteristics specified in the Section 7.3.2 to discover the process window with the ideal parameters for Compaction force and Heat level. To begin, the heat level was held constant while the compaction force was adjusted, with the optimal value $Q_m$ assigned to see how increasing or reducing this value affected the results. The other samples are created in the same way but with the compaction force value fixed and changing the heat level.

| | $F_{\text{lower}}$ | $F_{\text{M}}$ | $F_{\text{upper}}$ |
|---|---|---|---|
| $Q_{\text{lower}}$ | | ○ | |
| $Q_{\text{M}}$ | ● | ○ ● | ● |
| $Q_{\text{upper}}$ | | ○ | |

Table 3: Testing matrix.
• shows tests where heat level remains constant;
○ shows tests where compaction force is fixed.

The heat levels $Q_{\text{lower}}$, $Q_{\text{M}}$, and $Q_{\text{upper}}$ are measured in nanoliters per minute of the mixture of gases Oxygen, hydrogen, and air. Within the initial configuration, the percentage of these two of the total flow for the quantity of air is feasible, for example, 100% of the gas mixture will give us a total of zero nanoliters per minute of air, and if this number decreases, the flow control valves will let air into the system. The ratio between hydrogen and oxygen, on the other hand, will always be 2: 1 as previously stated.

The following heat levels were employed to perform the tests:

- Heat level 3: 3 nL/min ; $Q_{\text{lower}}$
- Heat level 4: 4 nL/min ; $Q_{\text{M}}$
- Heat level 5: 5 nL/min ; $Q_{\text{upper}}$

Likewise, the taping tool software allows to vary the force, having a maximum limit set at 300 N. The following values were established for the tests:

- $F_{\text{lower}}$: 150 N
- $F_{\text{M}}$: 200 N
- $F_{\text{upper}}$:250 N

## 7.4 Tensile Test setup

For the tests performed in this section, the guidelines established in Standard ISO 527 part I, II, III and IV and ISO 11339, respectively, were followed, using the universal tester machine Instron equipped with a max load of 100KN shown in Fig. 35.

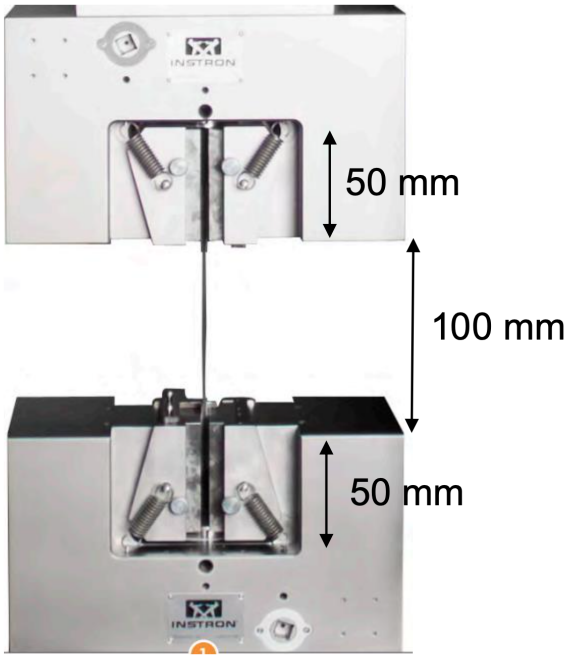


Figure 35: Universal tester machine used for testing

The setup of each test described in the Table 1, as well as the findings achieved, will be shown in this section. Just after that, there will be a general discussion followed by some recommendations.

### 7.4.1 Single Lap Shear test - Test A

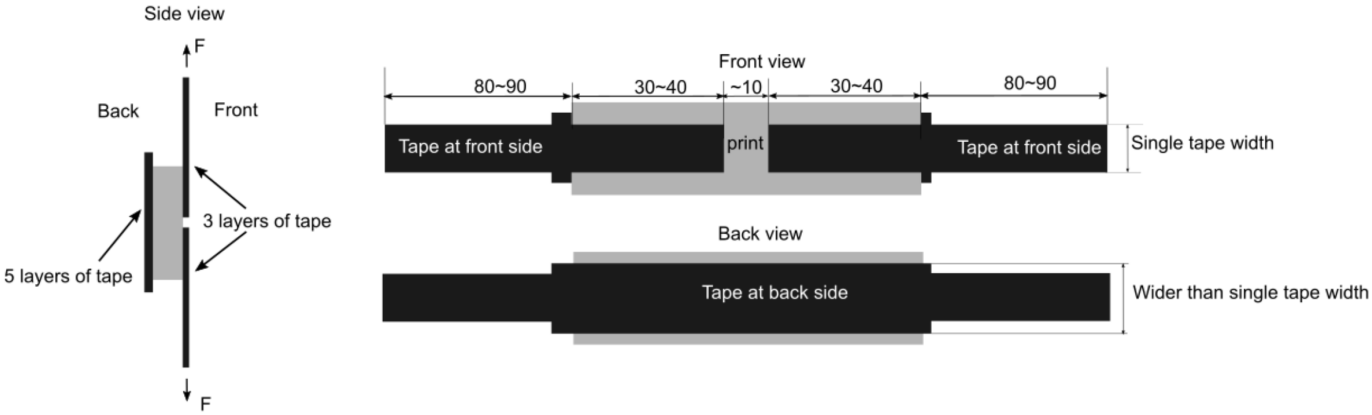


Figure 36: Test A specimen dimensions

For this test, two types of configurations were employed; the dimensions for the specimen fabrication are indicated in Fig. 36. The difference between the two configurations can be seen in Fig. 37, where configuration one is the same as the specimen shown above and configuration two is obtained after performing a first tensile test where one tape is already detached.

In summary:

- Configuration 1: Tape to tape clamped tensile test
- Configuration 2: Tape to Print clamped tensile test

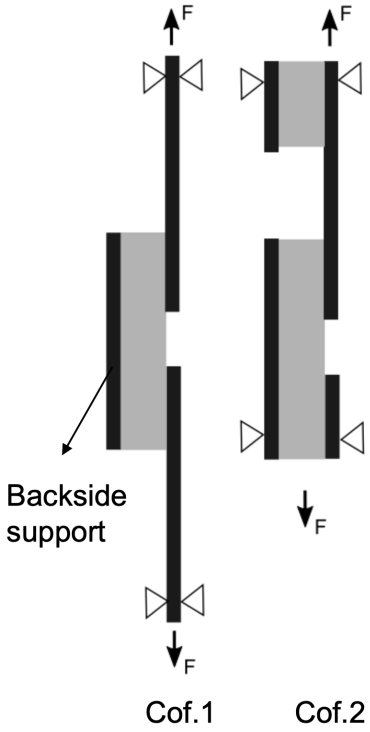


Figure 37: Test A specimen configuration 1 and 2

The purpose of this test is to determine the bonding strength in the cross-section area between the tape and the printed element. For tapes that peel off after testing, the overlap shear strength is measured given the actual bonding length or $L_{nominal}$, as shown in Fig. 38. To calculate the Lap shear strength Eq. (1).

$$LapShearStrength = \frac{F_{max}}{L_{nominal} \cdot W_{tape}} \tag{1}$$

Where:

- $F_{max}$: Force at debonding
- $L_{nominal}$: Bonding length
- $W_{tape}$: Tape width, 6 or 10 mm

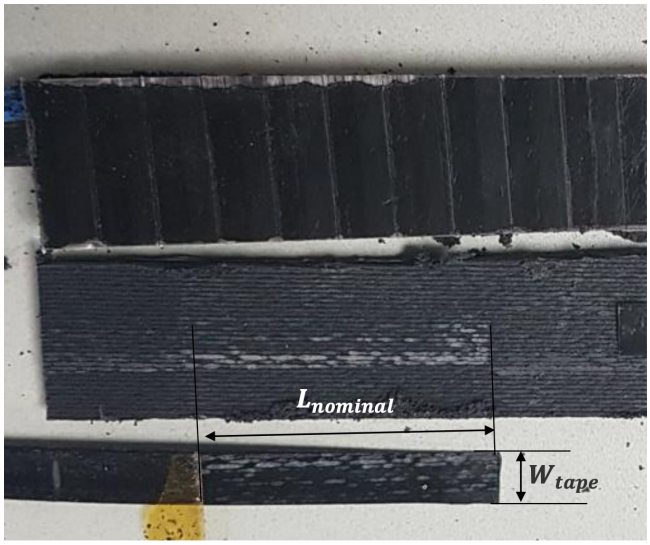


Figure 38: Cross-sectional bonding area

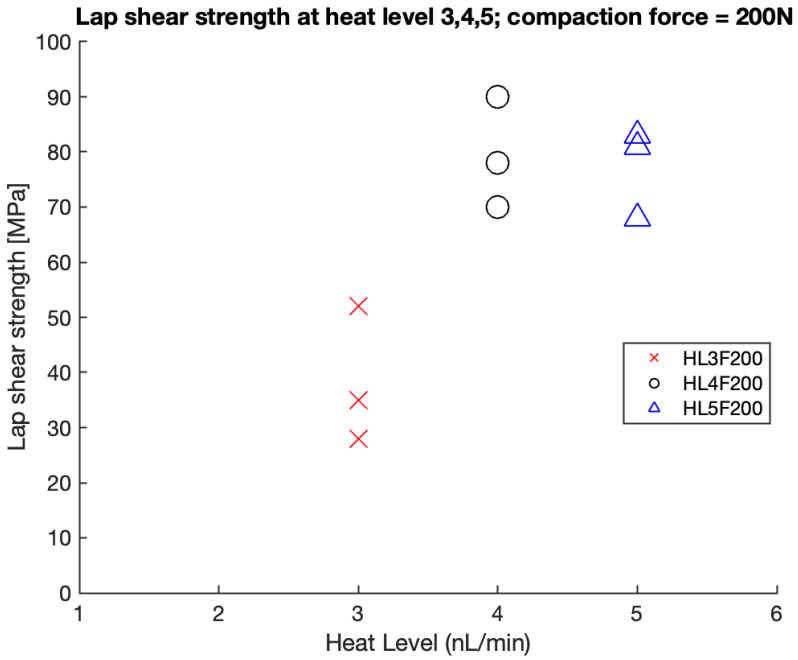


Figure 39: Heat level changing - Compaction Force fixed results

From Fig. 39 it is possible to deduce that Heat Level 4 and Heat Level 5 provide stronger print to tape bonding, compared to Heat Level 3, while the results in Fig. 41 imply that the smaller the compaction force, it produces a stronger bond. This opposes the results obtained by Çelik for laser-assisted fiber placement, where the tests show an evident proportional relationship between the compaction force and the degree of effective intimate contact. [15]

The previously discussed lack of performance compared to the laser-assisted process can be explained by the highly uneven printed surface, which results in an effective print-tape bonding area concentrated only at the peaks of the printed profile, as observed in Fig. 40. As a result of the non-flatness of the printed substrate and the hardness of the roller, the bonding region

beneath the tape is not consistent, and the gaps between the printed layers are not completely filled.

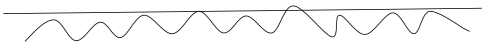

Figure 40: Test A boding results

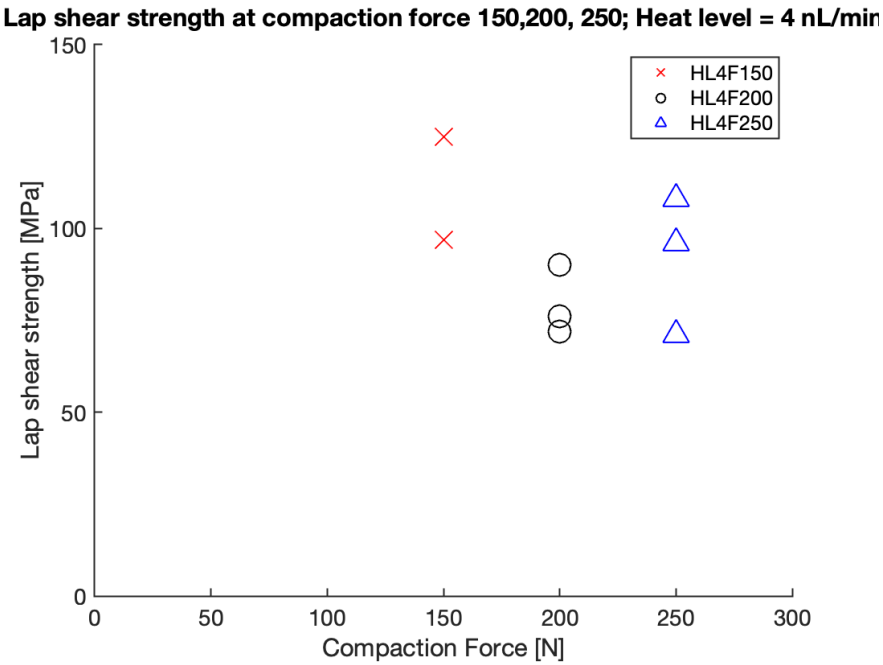


Figure 41: Compaction force changing - Heat level fixed results

Due to the bending nature of the samples, two components were discovered throughout the tests: shear and peeling, indicating a low-quality print part. Fig. 42a shows how the specimen's curvature causes the test to be misaligned, requiring the first phase to stretch the part before performing the real single lap shear test.


(a) Test A specimen before loading configuration 1

(b) Test A result configuration 1

Figure 42

### 7.4.2 Peeling Test - Test B

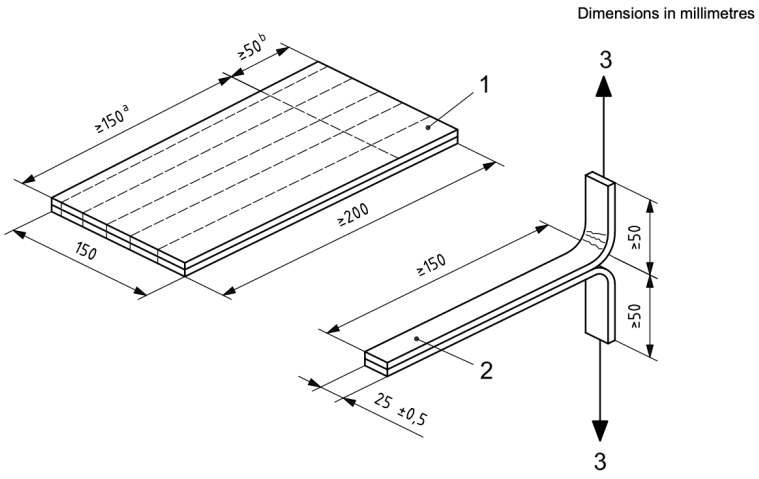


Figure 43: Test B specimen dimensions ISO 11339:2010

To carry out Test B, the dimensions specified in *EN ISO 11339: 2010 T-peel test for flexible-to-flexible bonded assemblies* were followed, Fig. 43. Consisting of three layers of tape added to each side for a total of six plies, and a 70-100 mm opening at one end to attach to the universal tester's crossheads. The tape is 10 mm wide rather than 25 mm because it is an off-the-shelf product from the tape manufacturer. As seen in Fig. 44, this is the only substantial difference between the actual measurements and the ones defined by the standard.

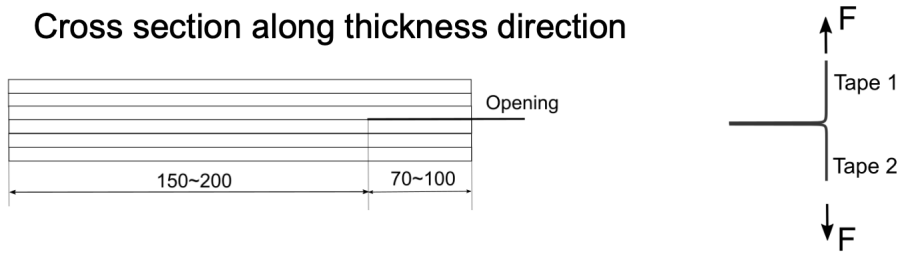


Figure 44: Test B specimen dimension in mm adapted from standard ISO 11339:2010 with 10 mm width

As a consequence of the low peeling speed, the tapes are bent and broken first, followed by interfacial peeling; as the crossheads translate, the tapes are bent and broken again at a new point, therefore the test speed had to be increased to 70 mm/min. The peaks in the first test run at 10 mm/min found in the Fig. 45 clearly demonstrate the effects of the bending, while the valleys immediately after are the true peeling component at around 10 N. It was discovered that as the test speed is increased, the bending effect decreases, as demonstrated in specimen 2. The rest of the results of the samples presented in Fig. 47b were done at 70 mm/min since better results were obtained at this rate.

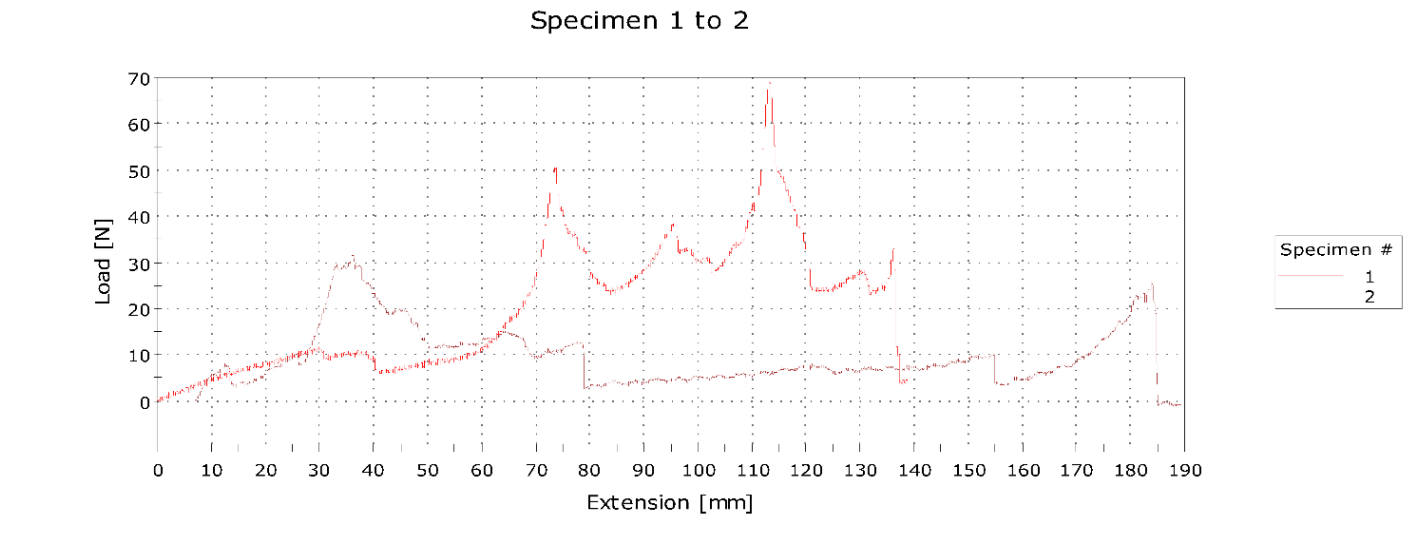


Figure 45: Test B results, specimen 1 tested at 10 mm/min and specimen 2 at 50 mm/min

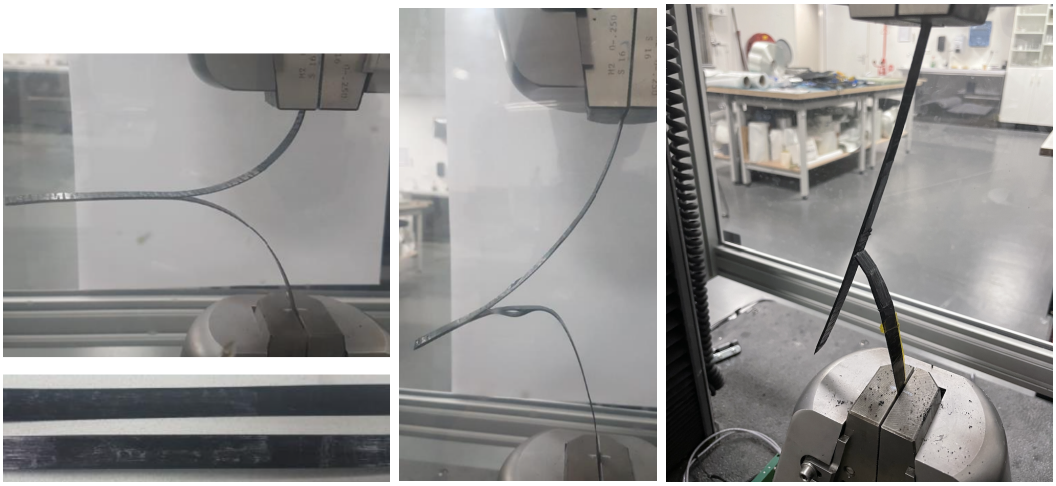

(a) Initial Setup (b) Before failure (c) After failure

Figure 46: Peeling Setup and Failure

After the placing process, the samples stiffened due to thermal stresses within the tape, and thus during the initial setup for the test was difficult to prevent damaging the specimens. In Fig. 46a, the adhesive tape to tape part of the sample is in horizontal orientation, indicating the test's initial position. The bonded section tends to tip downwards after the crossheads have traveled and before the failure occurs, Fig. 46b. Finally, when the sample fails, it breaks, detaching totally from the bonded area at some point, as shown in Fig. 46c.

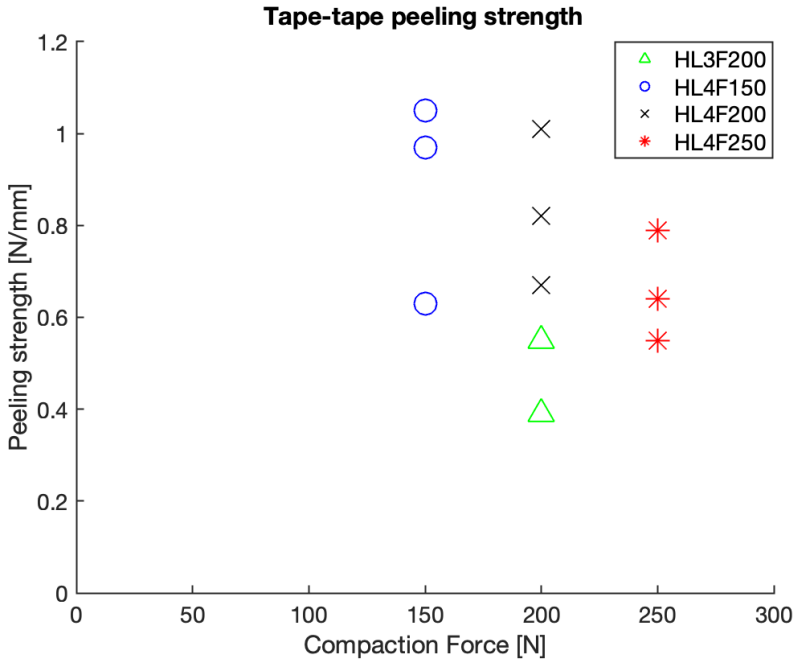


(a) Tape-Tape peeling strength

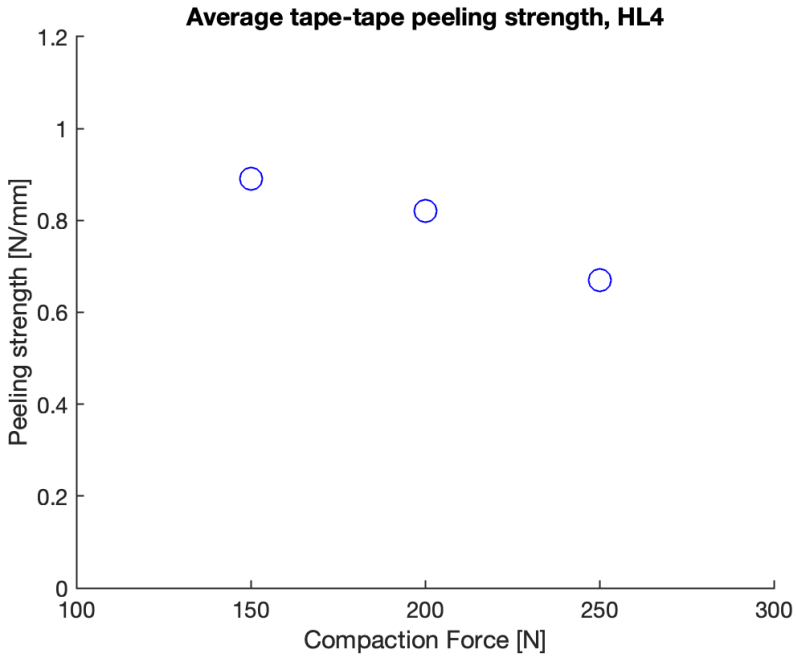


(b) Average Tape-Tape peeling strength with Heat level 4 (nL/min)

Figure 47: Peeling strength results

The results of the peeling test displayed in Fig. 47 establish a greater influence by the heat level than the one produced by the compaction force. In this case, the results could be explained by the lack of heat transfer to overcome the glass transition temperature so the polymer matrix of the tape can adhere to the previous layer of tape. Results given by Çelik demonstrate a similar case scenario where the compaction force benefits the adhesion but there is a threshold where it doesn't enhance anymore and starts affecting negatively.

While in Fig. 48a it can be seen how the 3 specimens with the same configuration of Heat level 4

and Compaction force 150 N failed to stabilize and proceeded straight to failure. The expected outcome was that the tape would exhibit an obvious steady state where failure patterns could be seen before this occurred.

In conclusion, there is no substantial difference in peeling strength across compaction forces, however, Heat level 4 [nL/min] yields better bonding strength than Heat level 3 [nL/min] with the same compaction force.

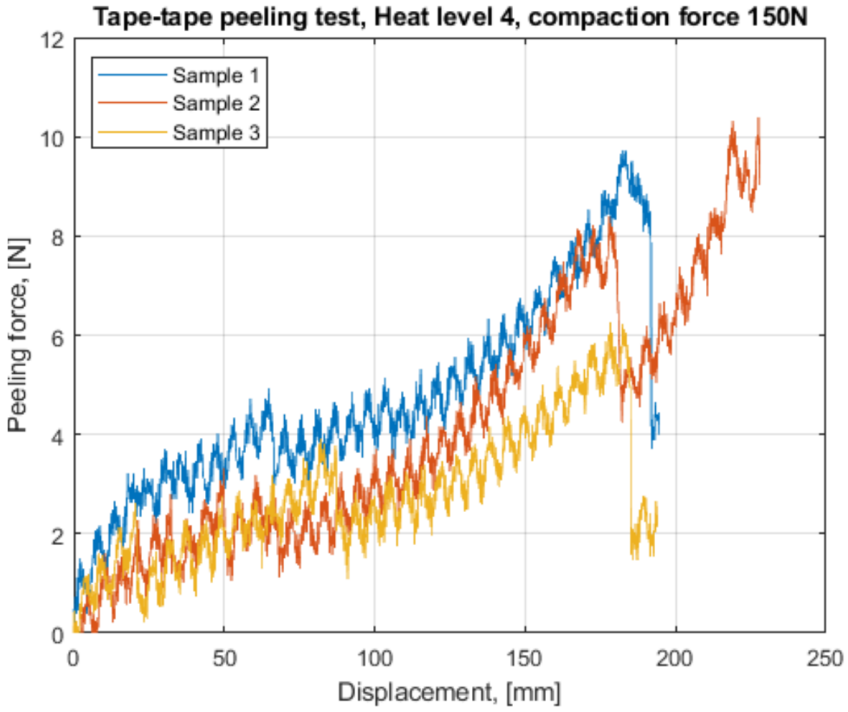


(a) Tape-Tape peeling force vs Displacement graph

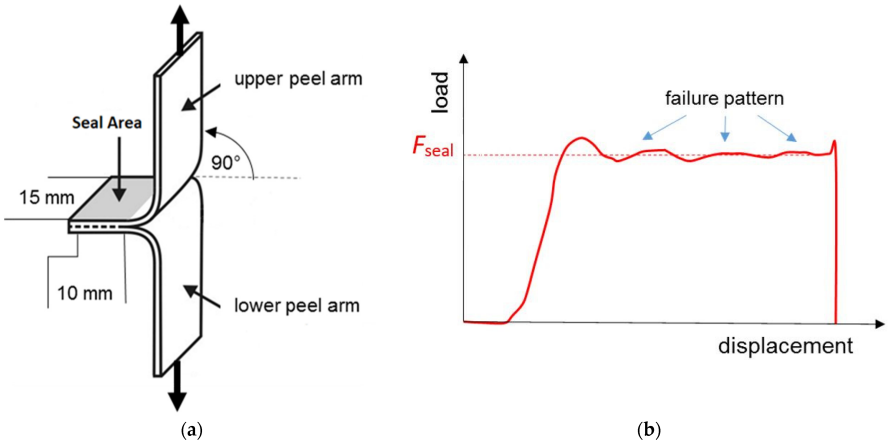


(b) Expected Peeling force vs Displacement graph [8]

Figure 48: Peeling strength results

### 7.4.3 Taping Angle Study - Test C

The primary goal of this test is to see if the bonding strength varies depending on the angle at which the tape is applied. The tape was placed at 0°, 45°, and 90°orientations, as seen in the following image.

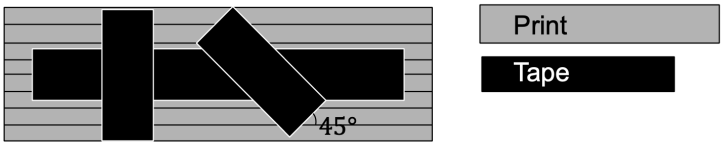


Figure 49: Test C specimen orientations, horizontal tape is considered as $0^{o}$, vertical tape as $90^{o}$ and $45^{o}$ in diagonal orientation.

For this test, the next specifications were followed:

1. At $v_{max}$ , $Q_m$ and $F_m$ , test 0°, 45° and 90° taping angle relative to the printing direction.
2. The configuration of single lap shear sample is the same as test A.
3. 3 samples for each angle, and 9 samples in total for test C.

| | $v_{max}$ , $Q_m$ and $F_m$ |
|---|---|
| 0° | • |
| 45° | • |
| 90° | • |

Table 4: Samples configuration for testing taping angles

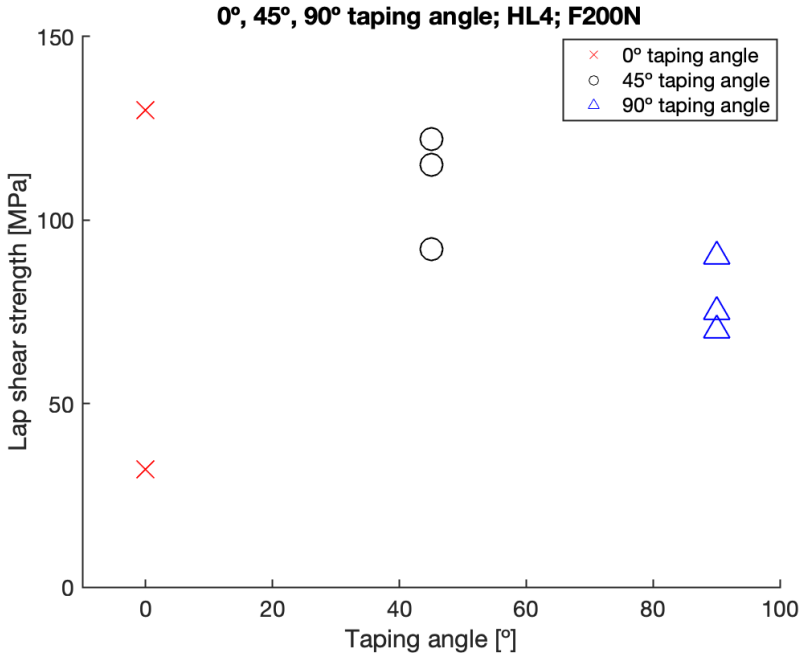


Figure 50: Taping angle results

The following conclusions can be drawn from the results shown in Fig. 50:

- The bonding area is not uniform underneath the tape due to the non- flatness of the printed substrate and the hardness of the roller. This is more obvious for the 0°print-tape profile in Fig. 51.

- Samples are highly deformed due to taping towards the backside of the print. Taping at 90° produces the most bending deformation compared with 0° and 45° taping. Due to the deformation, the test combines the lap shear test with the peeling test.
- When the taping angle is perpendicular to the printing angle, the print-tape bonding strength is higher than the printed substrate itself, around 10 MPa. When the taping angle is the same as the printing angle, the printed material is still stronger than some of the print-tape bonding strengths. These strengths are still far away from the strength of the moulding produced parts. By adding more plies of tapes, it is expected to get a comparable strength.
- There is a significative better performance at a 45°taping angle compared to the 90°due to the non-uniformity of the surface. The expected results with a perfectly uniform surface would throw that there is not a substantial difference between the angles since the effective contact area among them is almost the same.

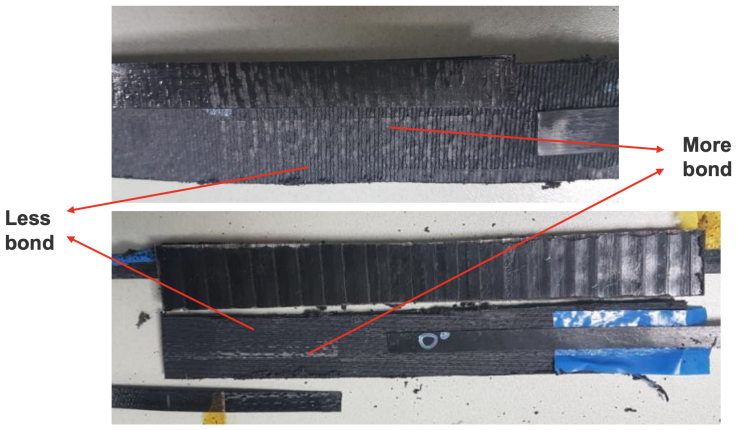


Figure 51: Test C bonding results

### 7.4.4 Tape Tensile strength - Test D

This test was carried out using a configuration similar to TEST B, with the tape clamped at each end for each of the two variants: 6 mm and 10 mm, see Fig. 52. Here are the characteristics of the samples for this test:

1. Tensile test of tapes as received for both tape widths, 6 mm and 10 mm.
2. 3 samples for each tape width, 6 samples in total

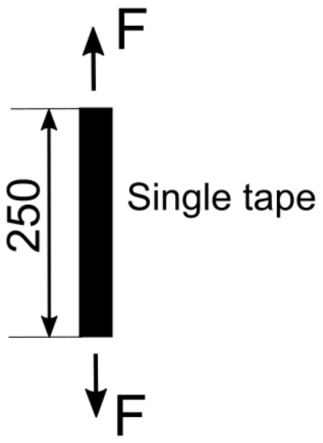


Figure 52: Test D specimen dimension

According to the results of Fig. 53, the 10 mm tape has a higher tensile strength. While the tensile strength should not be affected by the cross-sectional area, it is possible to identify a 50 percent increase in tensile strength for the 10 mm thickness. This could be explained by the crossheads' surface, having a large number of tiny teeth, that cut through the tape, causing a notch in the sample and a local weak point with a substantially stronger effect on the 6 mm tape.

Fiber characteristics, fiber volume %, and orientation all have a significant impact on longitudinal mechanical properties. The presence of fiber bundles rather than individual fibers also affects the tensile strength. For larger cross-sections, it can slightly increase because the atoms in the center become more constricted and therefore less responsive to the applied stress. [10]

Protective tabs must be added between the crossheads and the tape to prevent it from being damaged before the test even begins.

The manufacturer's specifications show a tensile strength of 1010 [MPa], but the average attained with the current configuration is around 500 [MPa]. After the clamping is enhanced with protecting tabs, it should be closer to 700 [MPa], which is comparable to the moulding test findings in Section 7.4.5

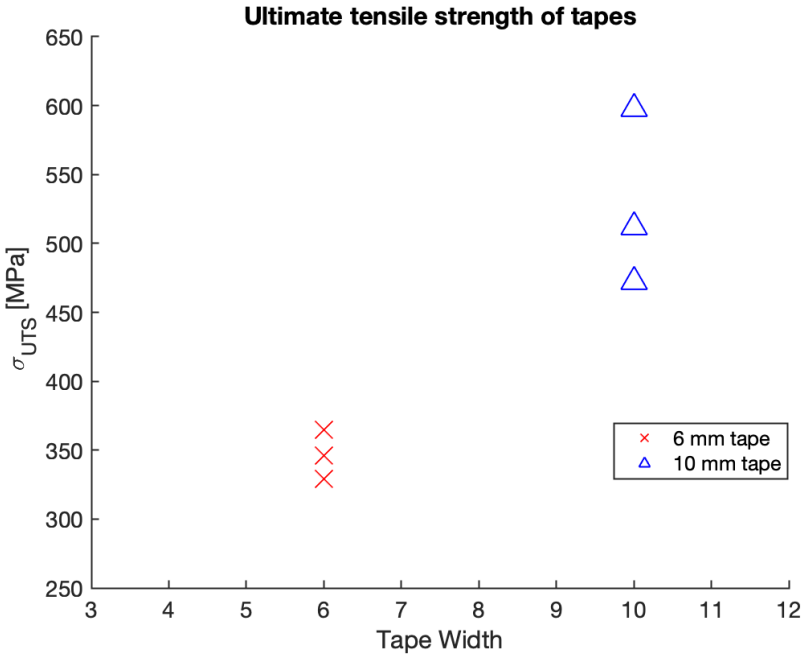


Figure 53: Test D $\sigma_{\text{UTS}}$ plot for 6 mm and 10 mm tape as coming from the manufacturer

### 7.4.5 Print-Tape bonding test - Test E

The goal of this test is to see if the tape-print bond strength can outperform the print interlayer strength once the tape is applied perpendicular to the print direction, as seen in Fig. 54. Previously, the tape was placed to the back of the printed panels to prevent them from breaking; however, in this test, the back support is not used.

Test E was performed with the following characteristics:

1. At $v_{max}$ , $Q_m$ and $F_m$ , taping direction perpendicular to the printing direction.
2. 3 layers of tapes.
3. 3 samples.

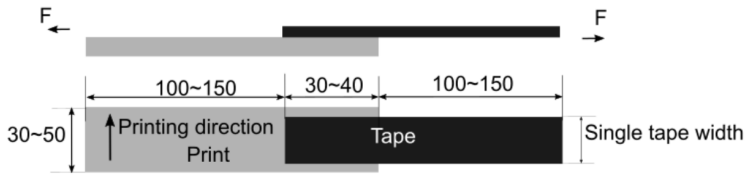


Figure 54: Test E specimen dimension

Once the tape is placed perpendicular to the printing direction, the printed material breaks during the lap shear test when it is not taped at the backside. The three samples for this test broke at the print part, so it can be concluded that the print-tape bonding strength, $> 25$ MPa, is greater than the interlayer bonding strength of the FDM-produced part, $\sim 10$ MPa.

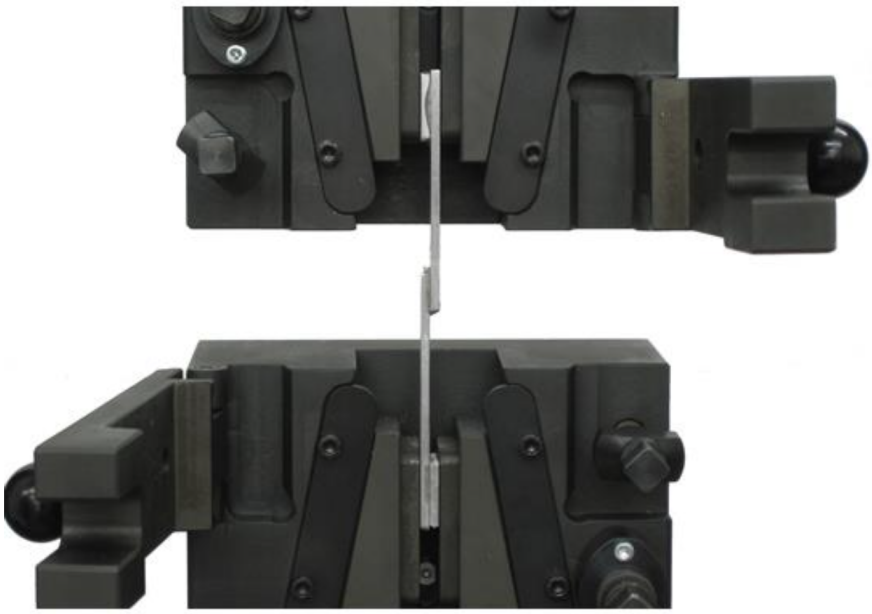

Figure 55: Test E specimen example

### 7.4.6 Moulding Part - Test F

To perform test F, rectangular samples were created using Hand layup UD Glass Fiber with polyester resin, Weight of GF, Wt% = 57%, fully cured in the oven at 100°C for 4 hours, and final Laminate thickness = 3.5mm. The goal of this test is to provide a benchmark for the combination of procedures. Stress-strain curves are presented in Fig. 56 to represent the mechanical properties of the molded material.

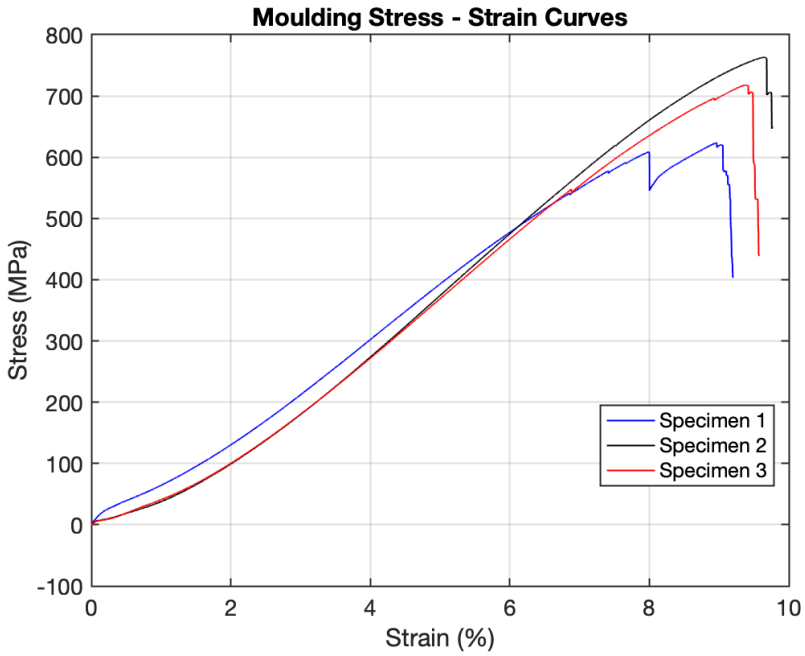


Figure 56: Moulding Stress - Strain graph

Since both the tape and the moulding are built of UD fibers, it makes it reasonable to compare them in the same graph. This is evident in the Fig. 57comparison. The tape strength expected with the improvements proposed in Section 7.4.4 would be similar to the one obtained for this test, as shown in this graph. However, the samples have a greater width, and it is worth noting that the tape strength expected with the improvements proposed in Section 7.4.4 would be similar to the one obtained for this test.

A more comprehensive comparison will be made in the Section 7.4.8, which will also cover the attributes of FDM-produced parts.

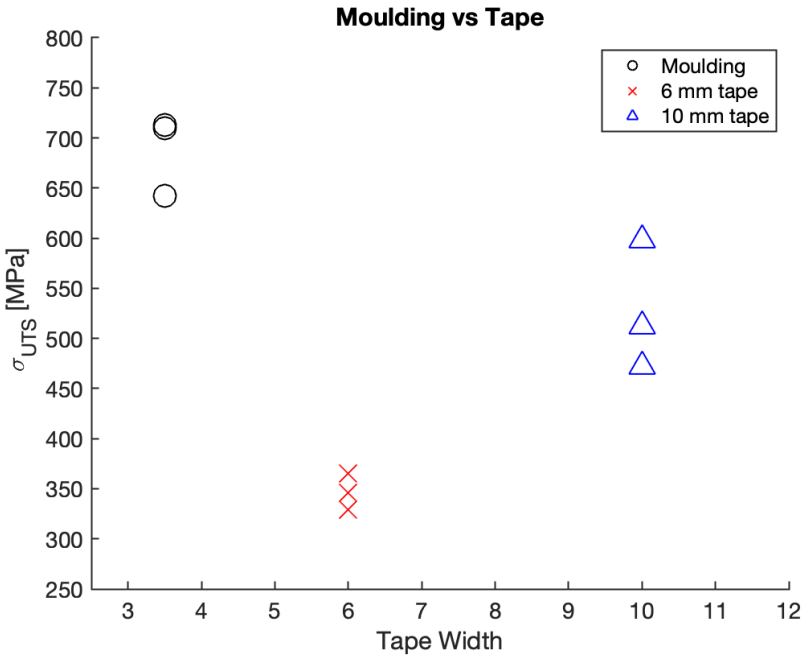


Figure 57: Tensile results for 13 mm wide moulding specimen compared to 6mm and 10mm width tape. Moulding produced part shows a better performance that the FDM printed part.

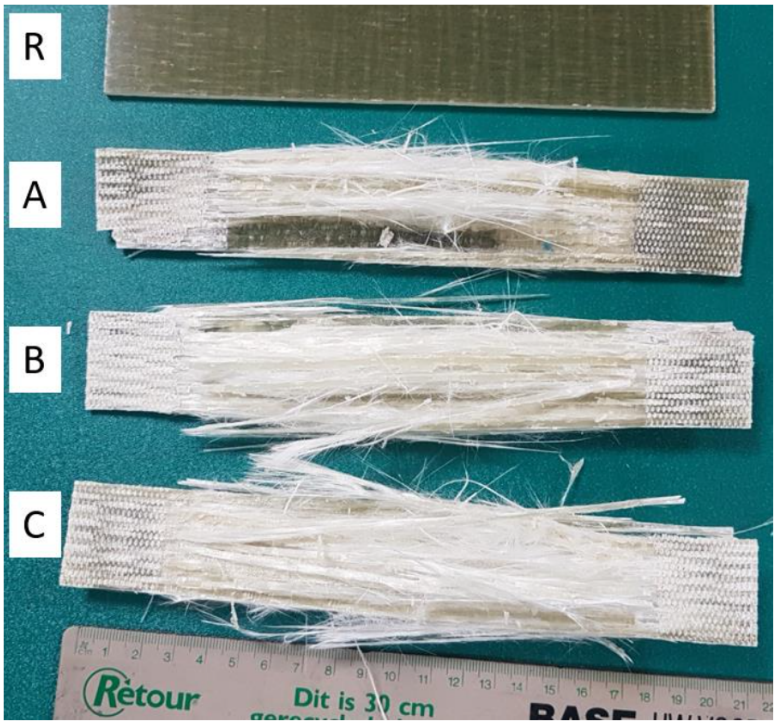


Figure 58: Moulding specimens after failing in the tensile test.

### 7.4.7 FDM Printing angle - Test G

This test seeks to capture the asymmetric properties inherent to the FDM process, as mentioned during Section 2.1. For this, shell cubes with a wall thickness of approximately 4 mm were printed at 10-xl facilities. The configuration of the tensile test samples is according to ISO 527-2: 2012 guidelines with angles of 0 °(along the printing direction), 45 °and 90 °(perpendicular to the printing direction) were extracted from these cubes using waterjet cutter with water pressure of around 3500 bars. The dimensions and orientations are presented in Fig. 59.

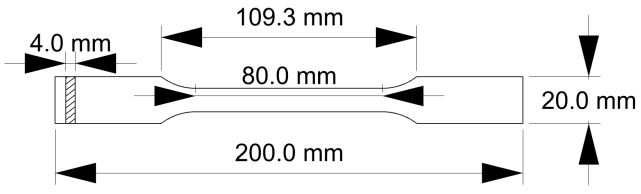


(a) FDM specimen dimensions according to ISO 527-2:2012 [26]

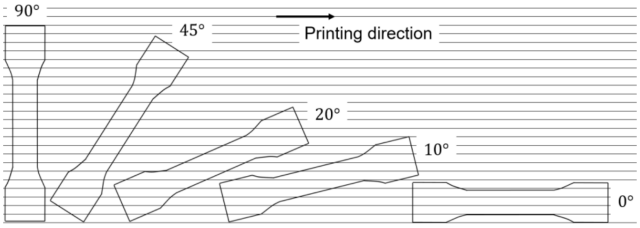


(b) FDM angle for testing specimens [8]

Figure 59

As noted in the previous sections, the specimen with a 0°profile yielded the greatest results, with an average of 33 MPa, while the specimen with a 90°profile yielded the worst results, with an average of roughly 10 MPa. While the printing angle approaches 90°, the tendency is negative to the strength, though nonlinear, as seen by the 45°orientation. It's worth noticing that for 45°and 90°, the failure shows alongside the printing angle, however for 0°, it appears perpendicular to the printing direction, as shown in the Fig. 61.

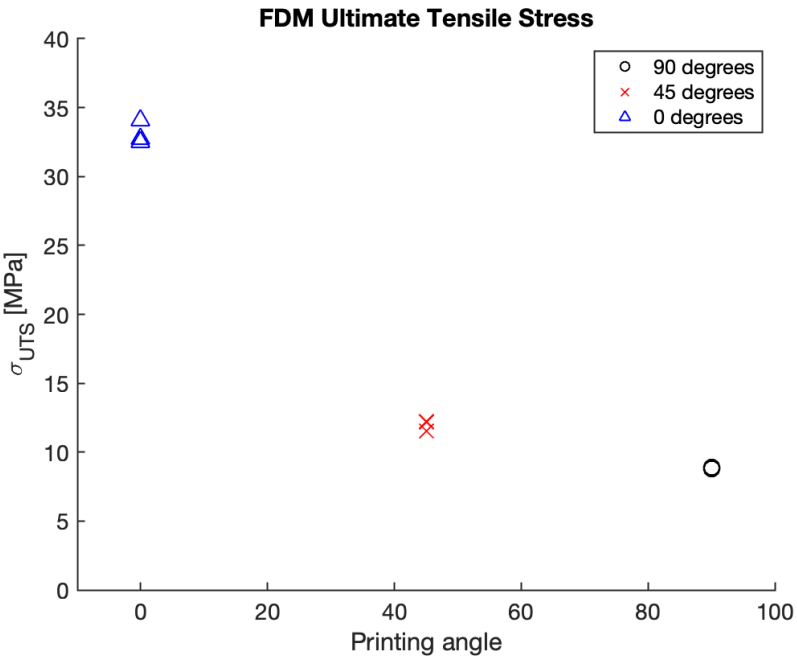


Figure 60: FDM Ultimate stress graph according to the printing angle

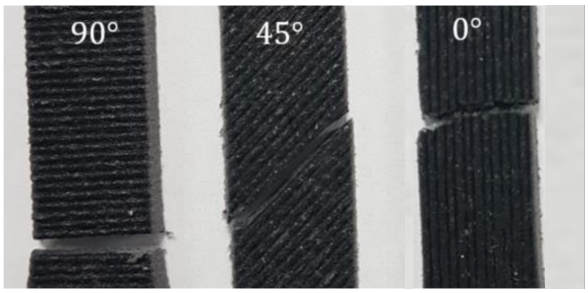


Figure 61: FDM specimens after failure after tensile test.

### 7.4.8 Discussion

The results shown in Section 7.4.6 and Section 7.4.7 for the current moulding and FDM processes make it clear that it is necessary to add the AFP process. Next, the main results obtained from the tests will be discussed to determine if with the selected parameters it is possible to equalize the properties of the current manufacturing process, as determined in research question 1. The effects were found by the adjustments of the different parameters as well as a comparison between them.

- The actual bonding area underneath the tape is not evenly distributed.

- The bonding strengths of the print-to-tape and tape-to-tape are both low. In the first scenario, the main cause is poor surface quality in terms of roughness and contact area. Nevertheless, the tape-to-tape lack of strength can be attributed to the heating source being too low, the matrix surface is not sufficiently melted, and there is scarcely any bonding.
- The compaction force seems less influence on the bonding strength than the heat level.
- The heat level 3 produces insufficient heat. Heat level 4 and 5 produce comparable bonding strength.
- 45° taping angle provides a higher bonding strength than 90° angle. 0° taping angle produces highly localized bonding area, with unreliable result.
- shear and peeling components were found during the single lap shear test due to the bending nature of the samples, which indicates the lack of quality of the specimens.
- The printed substrate is not perfectly leveled. This leads to uneven bonding cross the tape width.
- Peeling test contains bending as well due to the high stiffness of the tape.
- The tensile test of the tapes should be performed with protection tabs.

Using the values from Table 2 shown in Section 7.2. Where the transverse tensile modulus value for 3D printed PPGF30 (0.59 [GPa]) is lower than the moulding UD fabric (1.5 [Gpa]), making it less stiff and thus proving a clear weakness of the FDM part in the perpendicular orientation to the printing direction and illustrating the main reason for this research. [37]

However, to verify that adding the AFP process to FDM can resemble moulding, it is also necessary to compare longitudinal tensile modulus. In this case, the values are the following:

- FDM $E_{11} = 1.54$ [Gpa]
- Tape $E_{11} = 37$ [Gpa]
- Moulding fabric $E_{11} = 30$ [Gpa]

While the tensile strength of FDM combined with AFP parts should, in principle, be similar to that of the moulding fabric. It was observed during the tests that the print-to-tape bonding strength, 25 [MPa], and tape tensile strength, 350 [MPa] average for 6 mm tape and 550 [MPa] average for 10 mm, are still distant from the moulding process part strength, 700 [MPa].

RQ1 *Is it possible to overcome the drawbacks of Fused Deposition Modeling (FDM) adding Automated Fiber Placement (AFP) process?*

To address research question 1, consider $E_{11-\text{TAPE}}$ versus $E_{11-\text{MOULDING}}$ in the longitudinal direction, and $E_{22-\text{FDM}}$ against $E_{22-\text{MOULDING}}$ in the transversal direction, assuming an ideal bonding strength between print-tape-tape. This leads to the conclusion that while theoretically, similar performance is attainable, the current settings prevents these results from being reached for the time being.

Overall, there is a need to improve the surface contact area to increase the bonding strength. Three different strategies are proposed:

First, the surface quality must improve by adjusting the printing settings, nozzle diameter, printing speed, and layer height. Surface roughness can also be enhanced by adding CNC milling.

Second, warping can be prevented by adding a suction system to the working bed. Even though it is not possible to obtain entirely flat specimens after AFP due to thermal residual stresses induced to the printed part, the use of a thermal annealing post-process to reduce warpage should also be investigated.

Third, use a soft roller instead of a hard roller to prevent localized bonding area only at the peak between the layers of the FDM part. The usage of the soft roller will allow the tape matrix to reach the valley between layers and fill it with the substrate. This will increase the total bonding area.

Finally, heat transfer is not optimal at this moment, so the surface of the printed part and the tape are not sufficiently melted. The settings must be fine-tuned, and an infrared camera should be added to the setup to verify the current temperature of the substrate. In the case of the compaction force, no significant relationship between the variation in the different samples has been demonstrated.

# 8 Conclusion and Further steps

## 8.1 Conclusions

A combination of two current additive manufacturing techniques was investigated in this work to see if they may converge into a novel and enhanced process that could lead to mass industrial adoption. Starting with the foundations, state of the art, constraints, and restrictions, the gap and convenience of adding automated fiber insertion (AFP) to an increasingly popular production process were successfully established.

Nowadays, researchers are still looking for a technique to comprehend and theoretically anticipate the behavior of thermoplastic materials, but there is no consensus among the many studies. Each material has its unique set of values that were determined experimentally, yet there is always a difference in the results of each study. As previously stated, the results in this paper have room for improvement in terms of repeatability, this has to do with the parameters and situations under which both the impression and the tape insertion were performed.[11]

The most important observations are as follows:

- Given the manufacturer's technical parameters, the speed, temperature, and pressure utilized for 500mm/sec were successful, and the placement speed may be raised for the current setup and can be used in conjunction with FDM. With fine-tuned parameters and a soft roller, an optimal quality layup can be achieved.
- Between the trials carried out during this research and those carried out by Çelik and Leon et al., there is a clear difference in the relationship between the heat level, force compaction, and their response in the bonding strength.
- The taping tool manufacturer has achieved a maximum layup speed of 4 m/s using a fixed gantry configuration. With the current configuration at 10-XL including a robotic arm, a test was run at 750 mm/s, but due to the lack of appropriate parameters and

poor quality, the speed was reduced to 500 mm/s. In conclusion, the limiting factor is the robot and track speed rather than the ability to deliver the energy required.

## 8.2 Future steps

Future steps include a deeper analysis of the microscopic characteristics of the material, printed part roughness, tape-print bonding, and tape-tape bonding to study surface anomalies such as voids and fiber alignment over the cross-section, and a better understanding of the process parameters and the tape and printing material.

Second, new 'post-processes' or novel in-situ treatments, as proposed by [39] with 'repass' that is, simply reapplying temperature and consolidation pressure to the already laid laminate by repassing the AFP head on the laminate without adding any new material, while it has been studied for AFP in the aeronautical industry, could also be used in combination with FDM to improve surface quality.

# References


[1] ALL 3DP. All types of fdm 3d printers: Cartesian, corexy, & more). URL https://all3dp.com/2/cartesian-3d-printer-delta-scara-belt-corexy-polar/.

[2] ADDCOMPOSITES. Your complete solution provider for plug-and-produce afp systems. URL https://www.addcomposites.com/.

[3] Omid Aghababaei Tafreshi, S. Hoa, Farjad Shadmehri, Minh Duc Hoang, and Daniel Rosca. Determination of convective heat transfer coefficient for automated fiber placement (afp) for thermoplastic composites using hot gas torch. *Advanced Manufacturing: Polymer & Composites Science*, 6:1–15, 05 2020. doi: 10.1080/20550340.2020.1764236.

[4] M. Alex. The 4 types of fff / fdm 3d printer explained (cartesian, delta, polar). https://www.3dnatives.com/en/four-types-fdm-3d-printers140620174/#!, 2017. Accessed: 2021-10-06.

[5] ASTM. Astm f42/iso tc 261 develops additive manufacturing standards. https://www.astm.org/COMMIT/F42_AMStandardsStructureAndPrimer.pdf, 2017. Accessed: 2021-12-06.

[6] *Manual for F3-Compositor Application Unit.* AUTOMATION STEEG UND HOFFMEYER, 2021.

[7] Abdurrahman Aydin, Kahraman Fatih, and Vjekoslav Ivkovic. *CAN HUMAN BEINGS PRODUCE EVERYTHING? THE LIMITS OF THE 3D PRINTERS*, pages 137–151. 07 2019. ISBN 978-605-7852-97-7.

[8] Juliana V. C. Azevedo, Esther Ramakers-van Dorp, Berenika Hausnerova, and Bernhard Möginger. The effects of chain-extending cross-linkers on the mechanical and thermal properties of poly(butylene adipate terephthalate)/poly(lactic acid) blown films. *Polymers*, 13(18), 2021. ISSN 2073-4360. URL https://www.mdpi.com/2073-4360/13/18/3092.

[9] Mohammad Bahar and Michael Sinapius. A novel approach: Combination of automated fiber placement (afp) and additive layer manufacturing (alm). *Journal of Composites Science*, 2:42, 07 2018. doi: 10.3390/jcs2030042.

[10] Christophe Baley, Antoine Kervoëlen, Marine Lan, Denis Cartié, Antoine Le Duigou, Alain Bourmaud, and Peter Davies. Flax/pp manufacture by automated fibre placement (afp). *Materials & Design*, 94:207–213, 2016. ISSN 0264-1275. doi: https://doi.org/10.1016/j.matdes.2016.01.011. URL https://www.sciencedirect.com/science/article/pii/S0264127516300144.

[11] Anis Baz Radwan. Experimental analysis of the automated fiber placement manufacturing parameters for high and low tack prepreg material. Master's thesis, University of South Carolina, 2019.

[12] Marcus Brown. Overcoming z-axis strength limitations in 3d printed composite parts, 02 2020. URL https://www.mlc-cad.com/overcoming-z-axis-strength-limitations-in-3d-printed-composite-parts/.

[13] Flaviana Calignano, Diego Manfredi, Elisa Paola Ambrosio, Sara Biamino, Mariangela Lombardi, Eleonora Atzeni, Alessandro Salmi, Paolo Minetola, Luca Iuliano, and Paolo Fino. Overview on additive manufacturing technologies. *Proceedings of the IEEE*, 105(4): 593–612, 2017. doi: 10.1109/JPROC.2016.2625098.

[14] Thomas Campbell, Christopher Williams, Olga Ivanova, and Banning Garrett. Could 3d printing change the world? technologies, potential, and implications of additive manufacturing. 10 2011.

[15] O. Çelik. *Consolidation during laser assisted fiber placement: Heating, compaction and cooling phases*. PhD thesis, Delft University of Technology, 2021.

[16] Coriolis. The reference in automated fiber placement. URL `https://www.coriolis-composites.com/industries/`.

[17] Mark Cotteleer, Jonathan Holdowsky, and Monika Mahto. The 3d opportunity primer, the basics of additive manufacturing. 2013. URL `https://www2.deloitte.com/us/en/insights/focus/3d-opportunity/the-3d-opportunity-primer-the-basics-of-additive-manufacturing.html`.

[18] John Ryan C. Dizon, Alejandro H. Espera, Qiyi Chen, and Rigoberto C. Advincula. Mechanical characterization of 3d-printed polymers. *Additive Manufacturing*, 20:44–67, 2018. ISSN 2214-8604. doi: https://doi.org/10.1016/j.addma.2017.12.002. URL `https://www.sciencedirect.com/science/article/pii/S2214860417302749`.

[19] DPS-Software. Eureka. URL `https://www.dps-software.de/produkte/fertigung-cam/eureka`.

[20] Boris Fedulov. Modeling of manufacturing of thermoplastic composites and residual stress prediction. *Aerospace Systems*, 1, 11 2018. doi: 10.1007/s42401-018-0018-8.

[21] *Data Sheet UDMAXTM GPP 45-70 TAPE (0.25 mm)*. FRT TAPES, 2020.

[22] Wei Gao, Yunbo Zhang, Devarajan Ramanujan, Karthik Ramani, Yong Chen, Christopher B. Williams, Charlie C.L. Wang, Yung C. Shin, Song Zhang, and Pablo D. Zavattieri. The status, challenges, and future of additive manufacturing in engineering. *Computer-Aided Design*, 69:65–89, 2015. ISSN 0010-4485. doi: https://doi.org/10.1016/j.cad.2015.04.001. URL `https://www.sciencedirect.com/science/article/pii/S0010448515000469`.

[23] Chris Garrett. The best 3d printing slicer software roundup, 02 2020. URL `https://3dprinterchat.com/best-slicer-software/`.

[24] Ramy Harik, Clint Saidy, S J Williams, Zafer Gurdal, and B. Grimsley. Automated fiber placement defect identity cards: cause, anticipation, existence, significance,and progression. *SAMPE Conf Proc 2018.*, pages 1–16, 2018.

[25] Jigang Huang, Qin Qin, and Jie Wang. A review of stereolithography: Processes and systems. *Processes*, 8(9), 2020. ISSN 2227-9717. doi: 10.3390/pr8091138. URL `https://www.mdpi.com/2227-9717/8/9/1138`.

[26] ISO 527-2:2012. Plastics — determination of tensile properties – part 2: Test conditions for moulding and extrusion plastics. Standard, International Organization for Standardization, February 2012.

[27] ISO 527-2:2012. Plastics — determination of tensile properties – part 1: General principles. Standard, International Organization for Standardization, February 2012.

[28] Umme Kalsoom, Pavel N. Nesterenko, and Brett Paull. Recent developments in 3d printable composite materials. *RSC Adv.*, 6:60355–60371, 2016. doi: 10.1039/C6RA11334F. URL http://dx.doi.org/10.1039/C6RA11334F.

[29] David Kazmer. 28 - three-dimensional printing of plastics. In Myer Kutz, editor, *Applied Plastics Engineering Handbook (Second Edition)*, Plastics Design Library, pages 617–634. William Andrew Publishing, second edition edition, 2017. ISBN 978-0-323-39040-8. doi: https://doi.org/10.1016/B978-0-323-39040-8.00029-8. URL https://www.sciencedirect.com/science/article/pii/B9780323390408000298.

[30] Angel Leon, Clara Argerich, Anais Barasinski, E. Soccard, and Francisco Chinesta. Effects of material and process parameters on in-situ consolidation. *International Journal of Material Forming*, 12, 07 2019. doi: 10.1007/s12289-018-1430-7.

[31] Markforged. Metal x™ system. URL https://markforged.com/3d-printers/metal-x.

[32] Isabel Martin, Diego Saenz-Castillo, Antonio Fernandez, and Alfredo Güemes. Advanced thermoplastic composite manufacturing by in-situ consolidation: A review. *Journal of Composites Science*, 4:149, 10 2020. doi: 10.3390/jcs4040149.

[33] Tuan D. Ngo, Alireza Kashani, Gabriele Imbalzano, Kate T.Q. Nguyen, and David Hui. Additive manufacturing (3d printing): A review of materials, methods, applications and challenges. *Composites Part B: Engineering*, 143:172–196, 2018. ISSN 1359-8368. doi: https://doi.org/10.1016/j.compositesb.2018.02.012. URL https://www.sciencedirect.com/science/article/pii/S1359836817342944.

[34] Megan Nichols. When should you combine 3d printing and cnc machining?, 07 2019. URL https://www.fabbaloo.com/2019/07/when-should-you-combine-3d-printing-and-cnc-machining.

[35] Ebrahim Oromiehie. *In-situ process monitoring in automated fibre placement-based manufacturing of advanced composites*. PhD thesis, THE UNIVERSITY OF NEW SOUTH WALES, 2017.

[36] Felix Raspall, Rajkumar Velu, and Nahaad Mohammed Vaheed. Fabrication of complex 3d composites by fusing automated fiber placement (afp) and additive manufacturing (am) technologies. *Advanced Manufacturing: Polymer & Composites Science*, 5(1):6–16, 2019. doi: 10.1080/20550340.2018.1557397. URL https://doi.org/10.1080/20550340.2018.1557397.

[37] H.A. Rijsdijk, M. Contant, and A.A.J.M. Peijs. Continuous-glass-fibre-reinforced polypropylene composites. 1. influence of maleic-anhydride-modified polypropylene on mechanical properties. *Composites Science and Technology*, 48(1-4):161–172, 1993. ISSN 0266-3538.

[38] P.C. Sai and S. Yeole. Fused deposition modeling—insights. *International Conference on Advances in Design and Manufacturing, Bonfring*, pages 57–60, 2014. URL https://www.sciencedirect.com/science/article/pii/S0264127517302976.

[39] F. Shadmehri, S. Hoa, J. Fortin-Simpson, and Hossein Ghayoor. Effect of in situ treatment on the quality of flat thermoplastic composite plates made by automated fiber placement (afp). *Advanced Manufacturing: Polymer & Composites Science*, 4:1–7, 03 2018. doi: 10.1080/20550340.2018.1444535.

[40] Y. Song, Y. Li, W. Song, K. Yee, K.-Y. Lee, and V.L. Tagarielli. Measurements of the mechanical response of unidirectional 3d-printed pla. *Materials & Design*, 123:154–164, 2017. ISSN 0264-1275. doi: https://doi.org/10.1016/j.matdes.2017.03.051. URL https://www.sciencedirect.com/science/article/pii/S0264127517302976.

[41] 3D SOURCED. The 4 types of fdm 3d printer explained (cartesian, delta, polar & scara). URL https://www.3dsourced.com/3d-printers/types-of-fdm-3d-printer-cartesian-delta/.

[42] Ultimaker Support. What is g-code?, 03 2020. URL https://support.ultimaker.com/hc/en-us/articles/360012733080-What-is-g-code-.

[43] Daniyar Syrlybayev, Beibit Zharylkassyn, Aidana Seisekulova, Mustakhim Akhmetov, Asma Perveen, and Didier Talamona. Optimisation of strength properties of fdm printed parts—a critical review. *Polymers*, 13(10), May 2021. ISSN 2073-4360.

[44] *TRANSMARE® XP 2050-3D-01 TECHNICAL DATASHEET*. TRANSMARE COMPOUNDING, 2019.

[45] Sachini Wickramasinghe, Truong Do, and Phuong Tran. Fdm-based 3d printing of polymer and associated composite: A review on mechanical properties, defects and treatments. *Polymers*, 12(7), 2020. ISSN 2073-4360. doi: 10.3390/polym12071529. URL https://www.mdpi.com/2073-4360/12/7/1529.

[46] Tianyun Yao, Juan Ye, Zichen Deng, Kai Zhang, Yongbin Ma, and Huajiang Ouyang. Tensile failure strength and separation angle of fdm 3d printing pla material: Experimental and theoretical analyses. *Composites Part B: Engineering*, 188:107894, 2020. ISSN 1359-8368. doi: https://doi.org/10.1016/j.compositesb.2020.107894. URL https://www.sciencedirect.com/science/article/pii/S1359836819359396.

[47] A. Zeijen. Ecosystem emergence in the 3d printing industry. Master's thesis, Eindhoven University of Technology, 2015.

# A Appendices

## A.1 Appendix 1

TRANSMARE COMPOUNDING

### Technical Datasheet

**TRANSMARE® XP 2050-3D-01**
**3D printing compound Polypropylene, 50% glass fiber reinforced**

| General properties | Test method | Units SI | Typical value |
|---|---|---|---|
| **Shape** | Visual | | **Granular** |
| **Colour** | Visual | | **Translucent** |
| **Filling content** | Thermal analysis | % | **50** |

| Specific properties | Test method | Units SI | Typical value |
|---|---|---|---|
| **Density** | ISO 1183 | kg/m³ | **1330** |
| **Melt Flow Index** | ISO 1133 | | |
| at 230°C and 2,16 / 5,0 kg | | g/10 min | **2.5 / 8** |

| Mechanical properties | 1) | Test method | Units SI | Typical value |
|---|---|---|---|---|
| **Charpy impact strength** | | | | |
| unnotched, | at +23°C | ISO 179/1U | kJ/m² | **46** |
| unnotched, | at -40°C | ISO 179/1U | kJ/m² | - |
| notched, | at +23°C | ISO 179/1A | kJ/m² | **10** |
| notched, | at -40°C | ISO 179/1A | kJ/m² | - |
| **Izod impact strength** | | | | |
| unnotched, | at +23°C | ISO 180/1U | kJ/m² | - |
| unnotched, | at -40°C | ISO 180/1U | kJ/m² | - |
| notched, | at +23°C | ISO 180/1A | kJ/m² | - |
| notched, | at -40°C | ISO 180/1A | kJ/m² | - |
| **Tensile test** | | ISO 527-2 | | |
| tensile modulus | 2) | | MPa | **11700** |
| tensile stress at yield | 3) | | MPa | **125** |
| tensile stress at break | 3) | | MPa | **125** |
| elongation at yield | 3) | | % | **2.5** |
| elongation at break | 3) | | % | **2.5** |
| | 4) | | | |
| **Flexural test** | | ISO 178 | | |
| flexural modulus | | | MPa | **12000** |
| maximum flexural stress | | | MPa | **190** |
| **Hardness** | | ISO 868 | | |
| Shore D | | | - | **78** |

| Thermal Properties | Test method | Unit SI | Typical Value |
|---|---|---|---|
| **Heat deflection temperature** | | | |
| at 1.80 MPa (HDT/A ) | ISO 75/A | °C | **146** |
| at 0.45 MPa (HDT/B ) | ISO 75/B | °C | **157** |
| **Vicat softening point** | | | |
| at 10 N (VST/A) | ISO 306 | °C | **161** |
| at 50 N (VST/B) | ISO 306 | °C | **131** |

*1) Determined at injection molded test specimen*
*2) Test speed 1 mm/min, test specimen 4 mm thick*
*3) Test speed 50 mm/min, test specimen 4 mm thick*
*4) Three point bending; test speed 2mm/min*


Transmare Compounding B.V. | Ringweg 7 | 6045 JL | Roermond, The Netherlands|www.transmarecompounding.com
T: + 31(0)475 345 900 | E: compounding@transmare.nl

## A.2 Appendix 2


Data Sheet

# UDMAX™ GPP 45-70 TAPE (0.25 mm)

### DESCRIPTION

UDMAX™ GPP 45-70 TAPE is a UD glass reinforced, polypropylene based, composite material, produced using FRT's proprietary HPFIT™ technology, delivering optimal fiber spreading and a resin-rich surface layer at high fiber contents. UDMAX™ GPP 45-70 TAPE offers a combination of high strength and stiffness, which can result in weight reduction and overall customer product performance improvement. UDMAX™ GPP 45-70 TAPE is easily processable in tape weaving, winding, laying, lamination and other applications. Please contact our customer service department for available colors, tape length and width, as well as winding method.

### TYPICAL PROPERTIES VALUES

(Revision: 20200708)

| Name | Typical values | Unit | Test methods |
|---|---|---|---|
| PHYSICAL | | | |
| Matrix material | PP-H | | |
| Polymer melting point | 166 | °C | |
| Glass content | 45 | Volume% | - |
| Glass content | 70 | Weight% | - |
| Thickness | 0.250 | mm | - |
| Density | 1.67 | kg/dm$^3$ | ISO1183 |
| Areal weight | 417 | g/m$^2$ | - |
| MECHANICAL | | | |
| Tensile modulus 0° | 37 | GPa | ISO 527-5 |
| Tensile strength 0° | 1010 | MPa | ISO 527-5 |

### PROCESSING

It is not necessary to dry UDMAX™ GPP 45-70 TAPE prior to use. The recommended processing temperature range is 190° to 240°C. It is advised to allow newly shaped parts, produced using UDMAX™ GPP 45-70 TAPE, to cool down to 65°C or below, before further handling.

| | | | | Print dimensions | | | | Tape dimensions | | | | | |
|---|---|---|---|---|---|---|---|---|---|---|---|---|---|
| | Name | Heat level | Force level | length | width | width | thickness | length | width | thickness | Taping speed | Taping Angle | Strength to be studied |
| 1 | TEST A Qm-1a | 3 nl/min | 200 N | 90 mm | 30 | 30 mm | 4 mm | 120 mm | 10 mm | 0.25 mm | 500 mm/sec | 90º | Print-tape bonding |
| 2 | TEST A Qm-1b | 3 nl/min | 200 N | 90 mm | 30 | 30 mm | 4 mm | 120 mm | 10 mm | 0.25 mm | 500 mm/sec | 90º | Print-tape bonding |
| 3 | TEST A Qm-1c | 3 nl/min | 200 N | 90 mm | 30 | 30 mm | 4 mm | 120 mm | 10 mm | 0.25 mm | 500 mm/sec | 90º | Print-tape bonding |
| 4 | TEST A Qm-2a - Fm | 4 nl/min | 200 N | 90 mm | 30 | 30 mm | 4 mm | 120 mm | 10 mm | 0.25 mm | 500 mm/sec | 90º | Print-tape bonding |
| 5 | TEST A Qm-2b - Fm | 4 nl/min | 200 N | 90 mm | 30 | 30 mm | 4 mm | 120 mm | 10 mm | 0.25 mm | 500 mm/sec | 90º | Print-tape bonding |
| 6 | TEST A Qm-2c - Fm | 4 nl/min | 200 N | 90 mm | 30 | 30 mm | 4 mm | 120 mm | 10 mm | 0.25 mm | 500 mm/sec | 90º | Print-tape bonding |
| 7 | TEST A Qm-3a | 5 nl/min | 200 N | 90 mm | 30 | 30 mm | 4 mm | 120 mm | 10 mm | 0.25 mm | 500 mm/sec | 90º | Print-tape bonding |
| 8 | TEST A Qm-3b | 5 nl/min | 200 N | 90 mm | 30 | 30 mm | 4 mm | 120 mm | 10 mm | 0.25 mm | 500 mm/sec | 90º | Print-tape bonding |
| 9 | TEST A Qm-3c | 5 nl/min | 200 N | 90 mm | 30 | 30 mm | 4 mm | 120 mm | 10 mm | 0.25 mm | 500 mm/sec | 90º | Print-tape bonding |
| 10 | TEST A Fm-1a | 4 nl/min | 150 N | 90 mm | 30 | 30 mm | 4 mm | 120 mm | 10 mm | 0.25 mm | 500 mm/sec | 90º | Print-tape bonding |
| 11 | TEST A Fm-1b | 4 nl/min | 150 N | 90 mm | 30 | 30 mm | 4 mm | 120 mm | 10 mm | 0.25 mm | 500 mm/sec | 90º | Print-tape bonding |
| 12 | TEST A Fm-1c | 4 nl/min | 150 N | 90 mm | 30 | 30 mm | 4 mm | 120 mm | 10 mm | 0.25 mm | 500 mm/sec | 90º | Print-tape bonding |
| 13 | TEST A Fm-3a | 4 nl/min | 250 N | 90 mm | 30 | 30 mm | 4 mm | 120 mm | 10 mm | 0.25 mm | 500 mm/sec | 90º | Print-tape bonding |
| 14 | TEST A Fm-3b | 4 nl/min | 250 N | 90 mm | 30 | 30 mm | 4 mm | 120 mm | 10 mm | 0.25 mm | 500 mm/sec | 90º | Print-tape bonding |
| 15 | TEST A Fm-3c | 4 nl/min | 250 N | 90 mm | 30 | 30 mm | 4 mm | 120 mm | 10 mm | 0.25 mm | 500 mm/sec | 90º | Print-tape bonding |
| 16 | TEST B Qm-1a | 3 nl/min | 200 N | - | - | - | - | 120 mm | 10 mm | 0.25 mm | 500 mm/sec | 90º | Tape-tape bonding |
| 17 | TEST B Qm-1b | 3 nl/min | 200 N | - | - | - | - | 120 mm | 10 mm | 0.25 mm | 500 mm/sec | 90º | Tape-tape bonding |
| 18 | TEST B Qm-1c | 3 nl/min | 200 N | - | - | - | - | 120 mm | 10 mm | 0.25 mm | 500 mm/sec | 90º | Tape-tape bonding |
| 19 | TEST B Qm-2B - Fm | 4 nl/min | 200 N | - | - | - | - | 120 mm | 10 mm | 0.25 mm | 500 mm/sec | 90º | Tape-tape bonding |
| 20 | TEST B Qm-2b - Fm | 4 nl/min | 200 N | - | - | - | - | 120 mm | 10 mm | 0.25 mm | 500 mm/sec | 90º | Tape-tape bonding |
| 21 | TEST B Qm-2c - Fm | 4 nl/min | 200 N | - | - | - | - | 120 mm | 10 mm | 0.25 mm | 500 mm/sec | 90º | Tape-tape bonding |
| 22 | TEST B Qm-3a | 5 nl/min | 200 N | - | - | - | - | 120 mm | 10 mm | 0.25 mm | 500 mm/sec | 90º | Tape-tape bonding |
| 23 | TEST B Qm-3b | 5 nl/min | 200 N | - | - | - | - | 120 mm | 10 mm | 0.25 mm | 500 mm/sec | 90º | Tape-tape bonding |
| 24 | TEST B Qm-3c | 5 nl/min | 200 N | - | - | - | - | 120 mm | 10 mm | 0.25 mm | 500 mm/sec | 90º | Tape-tape bonding |
| 25 | TEST B Fm-1a | 4 nl/min | 150 N | - | - | - | - | 120 mm | 10 mm | 0.25 mm | 500 mm/sec | 90º | Tape-tape bonding |
| 26 | TEST B Fm-1b | 4 nl/min | 150 N | - | - | - | - | 120 mm | 10 mm | 0.25 mm | 500 mm/sec | 90º | Tape-tape bonding |
| 27 | TEST B Fm-1c | 4 nl/min | 150 N | - | - | - | - | 120 mm | 10 mm | 0.25 mm | 500 mm/sec | 90º | Tape-tape bonding |
| 28 | TEST B Fm-3a | 4 nl/min | 250 N | - | - | - | - | 120 mm | 10 mm | 0.25 mm | 500 mm/sec | 90º | Tape-tape bonding |
| 29 | TEST B Fm-3b | 4 nl/min | 250 N | - | - | - | - | 120 mm | 10 mm | 0.25 mm | 500 mm/sec | 90º | Tape-tape bonding |
| 30 | TEST B Fm-3c | 4 nl/min | 250 N | - | - | - | - | 120 mm | 10 mm | 0.25 mm | 500 mm/sec | 90º | Tape-tape bonding |
| 31 | TEST C - 0º 1 | 4 nl/min | 200 N | 90 mm | 40 | 40 mm | 4 mm | 120 mm | 10 mm | 0.25 mm | 500 mm/sec | 0º | Taping angle |
| 32 | TEST C - 0º 2 | 4 nl/min | 200 N | 90 mm | 40 | 40 mm | 4 mm | 120 mm | 10 mm | 0.25 mm | 500 mm/sec | 0º | Taping angle |
| 33 | TEST C - 0º 3 | 4 nl/min | 200 N | 90 mm | 40 | 40 mm | 4 mm | 120 mm | 10 mm | 0.25 mm | 500 mm/sec | 0º | Taping angle |
| 34 | TEST C - 45º 1 | 4 nl/min | 200 N | 90 mm | 40 | 40 mm | 4 mm | 120 mm | 10 mm | 0.25 mm | 500 mm/sec | 45º | Taping angle |
| 35 | TEST C - 45º 2 | 4 nl/min | 200 N | 90 mm | 40 | 40 mm | 4 mm | 120 mm | 10 mm | 0.25 mm | 500 mm/sec | 45º | Taping angle |
| 36 | TEST C - 45º 3 | 4 nl/min | 200 N | 90 mm | 40 | 40 mm | 4 mm | 120 mm | 10 mm | 0.25 mm | 500 mm/sec | 45º | Taping angle |
| 37 | TEST C - 90º 1 | 4 nl/min | 200 N | 90 mm | 40 | 40 mm | 4 mm | 120 mm | 10 mm | 0.25 mm | 500 mm/sec | 90º | Taping angle |
| 38 | TEST C - 90º 2 | 4 nl/min | 200 N | 90 mm | 40 | 40 mm | 4 mm | 120 mm | 10 mm | 0.25 mm | 500 mm/sec | 90º | Taping angle |
| 39 | TEST C - 90º 3 | 4 nl/min | 200 N | 90 mm | 40 | 40 mm | 4 mm | 120 mm | 10 mm | 0.25 mm | 500 mm/sec | 90º | Taping angle |
| 40 | TEST D - 6mm 1 | - | - | - | - | - | - | 250 mm | 6 mm | 0.25 mm | 500 mm/sec | - | Tape strength |
| 41 | TEST D - 6mm 2 | - | - | - | - | - | - | 250 mm | 6 mm | 0.25 mm | 500 mm/sec | - | Tape strength |
| 42 | TEST D - 6mm 3 | - | - | - | - | - | - | 250 mm | 6 mm | 0.25 mm | 500 mm/sec | - | Tape strength |
| 43 | TEST D - 10mm 1 | - | - | - | - | - | - | 250 mm | 10 mm | 0.25 mm | 500 mm/sec | - | Tape strength |
| 44 | TEST D - 10mm 2 | - | - | - | - | - | - | 250 mm | 10 mm | 0.25 mm | 500 mm/sec | - | Tape strength |
| 45 | TEST D - 10mm 3 | - | - | - | - | - | - | 250 mm | 10 mm | 0.25 mm | 500 mm/sec | - | Tape strength |
| 46 | TEST E - 1 | 4 nl/min | 200 N | 180 mm | 35 | 35 mm | 4 mm | 180 mm | 10 mm | 0.25 mm | 500 mm/sec | 90º | Print-tape bonding |
| 47 | TEST E - 2 | 4 nl/min | 200 N | 180 mm | 35 | 35 mm | 4 mm | 180 mm | 10 mm | 0.25 mm | 500 mm/sec | 90º | Print-tape bonding |
| 48 | TEST E - 3 | 4 nl/min | 200 N | 180 mm | 35 | 35 mm | 4 mm | 180 mm | 10 mm | 0.25 mm | 500 mm/sec | 90º | Print-tape bonding |